PLoS Pathogens

An insect serotonin receptor mediates cellular immune responses and its inhibition by phenylethylamide derivatives from bacterial secondary metabolites

Md Ariful Hasan[1], Hyun-Suk Yeom[2], Jaewook Ryu[2], Helge B. Bode[3], Yonggyun Kim[1,*]

[1] Department of Plant Medicals, College of Life Sciences, Andong National University, Andong 36729, Korea. [2] Center for Eco-Friendly New Materials, Korea Research Institute of Chemicals Technology, Yuseong, Daejeon 34114, Korea. [3] Department of Biosciences, Molecular Biotechnology, and Buchmann Institute for Molecular Life Sciences (BMLS), Goethe-Universität Frankfurt am Main, Germany

* Corresponding author: hosanna@anu.ac.kr

Abstract

Serotonin (5-hydroxytryptamine: 5-HT) is a biogenic monoamine that mediates immune responses and modulates nerve signal in insects. *Se-5HTR*, a specific receptor of serotonin, has been identified in the beet armyworm, *Spodoptera exigua*. It is classified into subtype 7 among known 5HTRs. *Se-5HTR* was expressed in all developmental stages of *S. exigua.* It was expressed in all tested tissues of larval stage. Its expression was up-regulated in hemocytes and fat body in response to immune challenge. RNA interference (RNAi) of *Se-5HTR* exhibited significant immunosuppression by preventing cellular immune responses such as phagocytosis and nodulation. Treatment with an inhibitor (SB-269970) specific to 5HTR subtype 7 resulted in significant immunosuppression. Such immunosuppression was also induced by bacterial secondary metabolites derived from *Xenorhabdus* and *Photorhabdus*. To determine specific bacterial metabolites inhibiting Se-5HTR, this study screened 37 bacterial secondary metabolites with respect to cellular immune responses associated with Se-5HTR and selected 10 potent inhibitors. These 10 selected compounds competitively inhibited cellular immune responses against 5-HT and shared phenylethylamide (PEA) chemical skeleton. Subsequently, 46 PEA derivatives were screened and resulting potent chemicals were used to design a compound to be highly inhibitory against Se-5HTR. The designed compound was chemically synthesized. It showed high immunosuppressive activities along with specific and competitive inhibition activity for Se-5HTR. This study reports the first 5HT receptor from *S. exigua* and provides its specific inhibitor designed from bacterial metabolites and their derivatives.

Author Summary

Serotonin (5-hydroxytryptamine: 5-HT) plays a crucial role in mediating nerve and immune signals in insects. Interruption of 5-HT signal leads to malfunctioning of various insect physiological processes. Se-5HTR, a 5-HT receptor of beet armyworm, *Spodoptera exigua*, was identified and classified as subtype 7 (5-HT_7) of 5-HT receptors. A specific inhibitor (SB-269970) for 5-HT_7 highly inhibited immune responses such as phagocytosis and nodulation mediated by Se-5HTR. Two entomopathogenic bacteria, *Xenorhabdus* and *Photorhabdus*, could secrete potent inhibitors against immune responses mediated by 5-HTR. Bacterial secondary metabolites were screened against Se-5HTR-mediating immune responses. Most of resulting compounds shared phenylethylamide (PEA) chemical skeleton. Subsequent screening using PEA derivatives supported the importance of this chemical skeleton. Based on their relative inhibitory activities, a compound was designed and synthesized. This novel compound possessed high inhibitory activities against Se-5HTR-mediating immune responses and exhibited competitive inhibition with 5-HT.

Introduction

Serotonin or 5-hydroxytryptamine (5-HT) is a biogenic monoamine found across most phyla of life [1]. This indolamine compound is biosynthesized from tryptophan by successive catalytic activities of tryptophan hydroxylase and aromatic-L-amino acid decarboxylase [2-4] primarily in nervous systems [5,6]. In human and other vertebrates, serotonin is a well-known neurotransmitter involved in mood, appetite, sleep, anxiety, cognition, and psychosis [7-9]. Outside the nervous system, serotonin plays important roles as growth factor and regulator of hemostasis and blood clotting [10,11]. In plants, serotonin is basically involved in stress signaling [12]. Serotonin plays crucial role in physiological and behavioral processes in insects and other invertebrates [13,14]. In *Drosophila melanogaster*, there is evidence that serotonin is required for courtship and mating [15], circadian rhythm [16,17], sleep [18], locomotion [13,19], aggression [20], insulin signaling and growth [21], and phagocytosis [22]. Serotonin is also involved in olfactory processing [23], feeding behavior [19], heart rate [24], and responses to light [25] in *D. melanogaster* larvae.

Serotonin modulates physiological processes by binding to specific receptors. Seven main subtypes of serotonin receptors have been classified in vertebrates [26]. Except 5-HT_3 receptor, the other six classes (5-HT_1, 5-HT_2, 5-HT_4, 5-HT_5, 5-HT_6, and 5-HT_7 receptors) belong to G protein-coupled receptor family [27]. Among these receptors, 5-HT_1 and 5-HT_5 receptors can inhibit cAMP synthesis by preferentially coupling to a trimeric G protein $G_{i/o}$ [28]. 5-HT_2 receptor uses $G_{q/11}$ to induce breakdown of inositol phosphates, resulting in an increase in cytosolic Ca^{2+} level [28]. Besides, 5-HT_4, 5-HT_6, and 5-HT_7 receptors coupled to G_s can stimulate cAMP production [28]. However, 5-HT_3 receptor is a ligand-gated cation channel that mediates neuronal depolarization [29].

79 Insects have at least three subtypes of 5-HT receptors. Five different 5-HT receptors as
80 orthologous to mammalian 5-HT_{1A}, 5-HT_{1B}, 5-HT_{2A}, 5-HT_{2B}, and 5-HT_7 have been identified in
81 *D. melanogaster* [14]. In addition, partial sequences of two 5-HT_1, two 5-HT_2, and one 5-HT_7
82 receptors have been identified in the field cricket *Gryllus bimaculatus* [30]. Two 5-HT_1 receptors
83 and two 5-HT_1 splice variants have been described in *Tribolium castaneum* and *Papilio xuthus*,
84 respectively [31,32]. As from *D. melanogaster* and *G. bimaculatus*, two 5-HT_2 receptors have
85 been described from *Apis mellifera* while only one 5-HT_2 receptor has been reported in other
86 insects such as *Periplaneta americana* and *Locusta migratoria* [33,34]. In a lepidopteran species,
87 *Pieris rapae*, four different 5-HT receptors including a novel subtype 8 have been reported
88 [35,36].

89 5-HT modulates various physiological processes via expression of different receptor types in
90 various tissues. 5-HT receptors are expressed highly in brain and ventral nerve cord of insects
91 [32]. 5-HT_1 receptor in honey bee brain is involved in visual information processing [37].
92 Expression pattern of 5-HT_7 receptor in honey bee nervous system suggests its possible roles in
93 information processing, learning, and memory [38]. 5-HT receptors might play roles in
94 neuroendocrine secretion and gut motility in cockroaches [29]. In salivary gland of several
95 insects, 5-HT_7 receptor has been reported to be involved in salivary secretion mediated by cAMP
96 level elevation [33,39,40]. Moreover, 5-HT_7 receptor mediates visceral muscle contraction in the
97 gastrointestinal tract of several insects including *A. aegypti* and *T. castaneum* [41,42]. 5-HT not
98 only has neurophysiological roles, but also mediates cellular immune responses in insects by
99 enhancing phagocytosis and nodulation [43]. Two different 5-HT receptors (1B and 2B) are
100 expressed in hemocytes of *P. rapae*, of which 5-HT receptor 1B mediates cellular immune
101 response [22]. In another lepidopteran insect, *Spodoptera exigua*, 5-HT mediates increase of total

102 circulatory hemocyte number by stimulating sessile hemocytes and mediating cellular immune
103 responses such as phagocytosis and nodule formation [44,45]. However, 5-HT receptor in *S.*
104 *exigua* has not been reported yet.

105 Two entomopathogenic bacteria, *Xenorhabdus* and *Photorhabdus*, can inhibit insect immune
106 responses to protect themselves and their symbiotic nematodes [46]. To accomplish host
107 immunosuppression, these bacteria can synthesize and secrete secondary metabolites to inhibit
108 immune signals and effectors [47]. Among these bacterial metabolites, tryptamine and
109 phenylethylamide derivatives have been identified with suggested function of interrupting 5-HT
110 signaling [48]. The objective of the present study was to determine bacterial secondary
111 compound(s) that could inhibit 5-HT signaling. To this end, we identified 5-HT receptor that
112 could mediate insect immunity in *S. exigua*. To determine a potent inhibitor of this receptor, we
113 screened bacterial secondary metabolites and their potent derivatives.

114

115 **Results**

116 **Bioinformatics analyses reveal that *S. exigua* contains a 5-HT receptor**

117 From a short read archive database (GenBank accession number: SRR1050532) of *S. exigua*, a
118 highly matched contig (accession number: GARL01017386.1) containing 3,308 bp nucleotide
119 sequence with an open reading frame (ORF) from 996th to 2,690th bp was identified. Prediction
120 of amino acid sequence by BlastP analysis revealed that its ORF sequence shared identities with
121 other insect 5-HT receptors: 99% with *Spodoptera litura* 5HTR (XP_022827337.1), 98% with
122 *Helicoverpa armigera* 5HTR (XP_021195909.1), 95% with *Trichoplusia ni* 5HTR
123 (XP_026729862.1), and 85% with *Manduca sexta* 5HTR (AGL46976.1). This novel 5-HT
124 receptor from *S. exigua* (Se-5HTR) encoded a sequence of 564 amino acids having a predicted

125 molecular weight of about 63.23 kDa. Phylogenetic analysis of its protein sequence indicated
126 that Se-5HTR was clustered with other 5-HT_7 receptors (Fig 1A). Predicted amino acid sequence
127 of Se-5HTR contained a signal peptide of 35 residues and attained GPCR character with seven
128 transmembrane domains. Consensus N-linked glycosylation sites are located in the N-terminus
129 (Asn^{48} and Asn^{53}), the third intracellular loop (Asn^{362}), and C-terminus (Asn^{534}). Several
130 consensus sites for phosphorylation by protein kinase A and/or protein kinase C were predicted
131 throughout the length of the sequence. A disulfide bond between two Cys residues at
132 extracellular matrix ('ECM', S1 Fig) is also predicted.

133 *Se-5HTR* sequence attains highly conserved amino acid residues (Fig 1B) found uniquely in
134 the biogenic monoamine receptor family [49-51]. Negatively charged Asp residue in TM3
135 (Asp^{163}) might interact with positively charged amino group of the ligand. A hydrogen bond
136 between the hydroxyl group of serine residue in TM5 (Ser^{247}) and the hydroxyl group of 5-HT
137 was predicted. In TM6, the consensus sequence unique to aminergic receptors (Phe^{444}-X-X-X-
138 Trp^{448}-X-Pro^{450}-X-Phe^{452}) is conserved. Like other GPCRs, a possible motif (Asn^{485}-Pro^{486}-X-X-
139 Tyr^{489}) that might participate in agonist-mediated sequestration and re-sensitization of Se-5HTR
140 is conserved in TM7. The C-terminus of the receptor contains two potential post-translational
141 palmitoylation cysteine residues (Cys^{508} and Cys-^{532}) and PDZ (post synaptic density protein,
142 *Drosophila* disc large tumor suppressor, and zonula occludens-1 protein)-domain binding motif
143 (Glu^{561}-Ser^{562}-Phe^{563}-Leu^{564}).

144

145 **Se-5HTR is expressed in all developmental stages and larval tissues**

146 Expression of *Se-5HTR* in different developmental stages of *S. exigua* was assessed by RT-PCR.
147 Results showed its expression from egg to adult stages (Fig 2A). RT-qPCR revealed variation in

148 its expression among developmental stages, with L5 larvae and adults showing the highest
149 expression levels. In L5 larvae, all tissues analyzed by RT-PCR showed its expression (Fig 2B).
150 RT-qPCR revealed that the midgut exhibited the highest expression level of *Se-5HTR*.
151 Hemocytes and brain also showed relatively high levels of its expression. Basal expression levels
152 of *Se-5HTR* were highly up-regulated in response to immune challenge (Fig 2C). *Se-5HTR*
153 expression was increased ~125-fold after challenge with fungus, *Beauveria bassiana* compared
154 to control (unchallenged). It was increased 60~90-fold after bacterial challenge compared to
155 naïve larvae.
156

157 **Specific inhibitors against 5-HTR suppress hemocyte behaviors of *S. exigua***

158 A commercial inhibitor (SB-269970) specific to 5-HT_7 was used to assess its effect on hemocyte
159 behaviors of *S. exigua* (Fig 3). Total hemocyte count (THC) of L5 larvae was ~1.2×10^7
160 cells/mL (Fig 3A). THC was significantly ($P < 0.05$) increased in response to 5-HT or bacterial
161 challenge. SB-269970 prevented the increase of THC in response to bacterial challenge. Its IC_{50}
162 value was estimated to be 1.925 μM. These results suggest that Se-5HTR can mediate hemocyte
163 mobilization in response to 5-HT upon bacterial challenge.

164 To determine the modulation effect of Se-5HTR on hemocyte-spreading behavior,
165 competitive inhibition between SB-269970 and 5-HT against Se-5HTR was assessed (Fig 3B).
166 Hemocytes were spread on slide glass with growth of F-actin. However, SB-269970 significantly
167 ($P < 0.05$) suppressed such hemocyte-spreading behavior. The inhibitory effect of the inhibitor
168 was rescued by addition of 5-HT. A relatively low dose (SB-269970: 5-HT = 10:1) of 5-HT did
169 not rescue the inhibitory effect. However, a relatively high dose (1:10) of 5-HT significantly ($P <$
170 0.05) rescued such inhibitory effect, indicating a specific competition between inhibitor and

171 ligand against Se-5HTR.

172

173 **RNA interference (RNAi) of Se-5HTR**

174 To address the immunomodulatory effect of Se-5HTR on hemocytes, its gene expression was
175 knocked-down by RNAi (Fig 4). RNAi was performed using dsRNA specific to *Se-5HTR*.
176 dsRNA-injected larvae exhibited significant ($P < 0.05$) reduction of *Se-5HTR* expression. RT-
177 qPCR analysis showed that about 90% of *Se-5HTR* mRNA was suppressed by dsRNA treatment
178 at 24 h PI (Fig 4A). At 24 h PI of dsRNA, *Se-5HTR* expression was analyzed in four different
179 tissue samples. Compared to control tissues, dsRNA-treated larvae exhibited significant ($P <$
180 0.05) reduction of *Se-5HTR* expression in all tissues including hemocytes.

181

182 **RNAi of Se-5HTR suppresses hemocyte behaviors of *S. exigua***

183 The effect of RNAi specific to Se-5HTR on hemocyte mobilization in response to bacterial
184 challenge was analyzed (Fig 4B). Upon bacterial challenge, THC increased by more than two
185 folds. However, RNAi treatment significantly ($P < 0.05$) suppressed such increase of THC. The
186 RNAi treatment also significantly ($P < 0.05$) influenced hemocyte-spreading behavior (Fig 4C).
187 On glass slide, hemocytes exhibited spreading behavior in 40 min by cytoskeletal rearrangement
188 through F-actin growth (see phalloidin staining). However, hemocytes collected from larvae
189 treated with RNAi specific to Se-5HTR lost such behavior.

190

191 **Modulation of cellular immune responses by Se-5HTR**

192 The influence of Se-5HTR on modulating hemocyte-spreading behavior suggested that it might
193 mediate cellular immune responses against bacterial infection. Phagocytosis against FITC-

194 labeled *Escherichia coli* was observed in hemocytes from control larvae. Labeled bacteria were
195 observed within hemocytes of control larvae (Fig 5A). However, hemocytes of larvae treated
196 with dsRNA specific to Se-5HTR significantly ($P < 0.05$) lost such phagocytosis, similar to that
197 found for hemocytes of larvae treated with SB-269970. Phagocytosis was decreased around 57%
198 or 78% after treatment with dsRNA or inhibitor, respectively. In response to bacterial challenge,
199 *S. exigua* formed ~78 hemocytic nodules per larva (Fig 5B). However, RNAi specific to Se-
200 5HTR or inhibitor treatment significantly ($P < 0.05$) reduced such cellular immune response.
201

202 **Influence of bacterial secondary metabolites on immune responses mediated by Se-5HTR**

203 RNAi or specific inhibitor assays indicated that 5-HTR could mediate both cellular immune
204 responses of phagocytosis and nodule formation in response to bacterial challenge. Bacterial
205 metabolites of two entomopathogens, *Xenorhabdus nematophila* (Xn) and *Photorhabdus*
206 *temperata temperata* (Ptt), were extracted from their culture broth using different organic
207 solvents and their inhibitory activities against cellular immune responses were then assessed (Fig
208 6). Organic solvent extracts of Xn- or Ptt-cultured broth exhibited significant ($P < 0.05$)
209 inhibitory activities against phagocytosis (Fig 6A) and nodulation (Fig 6B), although there were
210 variations in their inhibitory activities among extracts.

211 To identify bacterial secondary compounds that could inhibit Se-5HTR, 37 compounds (HB4
212 – HB602) derived from *Xenorhabdus* and *Photorhabdus* [47] were screened for their inhibitory
213 activities against hemocyte nodule formation and phagocytosis (Fig 7). More than three 75% (28
214 out of 37 compounds) of these test compounds exhibited significant ($P < 0.05$) inhibition against
215 phagocytosis (Fig 7A). In nodulation assay, all test compounds exhibited significant ($P < 0.05$)
216 inhibition (Fig 7B). Since Se-5HTR could mediate both cellular immune responses, bacterial

217 compounds that highly inhibited both phagocytosis (< 60%) and nodulation (< 30 nodules per
218 larva) were selected. As a result, 10 potent chemicals (HB 4, HB 5, H23, HB 30, HB44, HB 45,
219 HB 50, HB 223, HB 302, and HB 531) belonging to six chemical categories [phenylethylamide
220 (PEA), tryptamide, xenortide, xenocycloin, nematophin, and GameXPeptide] were found (S2
221 Fig). All these compounds exhibited median inhibitory concentration (IC_{50}) of 58~253 μM
222 against cellular immune response of hemocytic nodulation.

223 To support the specific inhibitory activity of these selected compounds against Se-5HTR,
224 competitive assay was performed between test compounds and 5-HT (Fig 8). With a constant
225 concentration of 5-HT, phagocytotic behavior of *S. exigua* hemocytes gradually decreased with
226 increasing amount of test compound (Fig 8A). On the other hand, increase of 5-HT amount
227 gradually decreased the phagocytotic behavior using a constant amount of test compound (Fig
228 8B).

229

230 **Influence of PEA derivatives on phagocytosis mediated by Se-5HTR**

231 These 10 selected compounds shared phenyl (or aromatic) ethylamide backbone except
232 xenocycloin (S2 Fig). Based on PEA backbone, 45 derivatives were selected from a chemical
233 bank and their inhibitory activities against the phagocytotic behavior of *S. exigua* hemocytes
234 were tested (Fig 9A). More than 66% (30 out of 45 compounds) of PEA derivatives exhibited
235 significant ($P < 0.05$) inhibition against phagocytosis. Three PEA derivatives (Ph15, Ph17, Ph33)
236 had inhibitory activities similar to a bacterial metabolite (HB 44), with IC_{50} at 1.8 ~ 5.6 μM
237 against phagocytosis (Fig 9B). These three PEA derivatives competitively inhibited the
238 phagocytosis mediated by Se-5HTR (Fig 9C).

239

240 **Synthesis of a potent inhibitor and inhibitory efficacy against Se-5HTR**

241 Potent compounds from 45 PEA derivatives were analyzed for their structures and activities
242 against phagocytosis mediated by Se-5HTR (S3 Fig). They shared the PEA backbone. However,
243 they had different side chains at 'X' and 'Y' (Fig S6A). When different X substituents were
244 compared for their inhibitory activities, methoxy was the most potent moiety (Fig S6B). When
245 different Y substituents were compared for their inhibitory activities with respect to identical X
246 groups, hexahydropyrrolo[1,2-a]pyrazine-1,4-dione was the most potent moiety (Fig S6C). This
247 analysis allowed us to design a hypothetical compound containing methoxy in X and
248 hexahydropyrrolo[1,2-a]pyrazine-1,4-dione at Y based on PEA backbone (Fig. S6D).

249 The designed compound ('PhX') was chemically synthesized and in its inhibitory activity
250 against phagocytosis was assessed compared with a specific 5-HT_7 inhibitor, SB269970, as a
251 reference (Fig 10). PhX was highly potent. It competitively inhibited cellular immune response
252 with 5-HT. Its inhibitory activity was more potent (t = 14.9; df = 32; P < 0.0001) than
253 SB269970.

254

255 **Discussion**

256 5-HT plays a crucial role in mediating cellular immune responses of *S. exigua* by stimulating
257 actin rearrangement [45]. Furthermore, it performs a functional cross-talk with eicosanoid
258 signaling via a small G protein Rac1 [52]. However, its signaling pathway leading to immune
259 responses remains unclear due to the lack of its receptor information in *S. exigua*. This study
260 identified a 5-HT receptor and showed its physiological function in mediating immune
261 responses.

262 Se-5HTR attains seven transmembrane domains and shares common molecular characters

263 with other 5-HT receptors. Like other GPCRs, Se-5HTR contains the canonical seven
264 transmembrane domains along with consensus glycosylation in the N-terminus (Asn^{48} and Asn^{53})
265 [53]. Additionally, its sequence contains a consensus aspartic acid residue in TM3 (Asp^{163}) and
266 a serine residue in TM5 (Ser^{247}) to interact with functional groups of biogenic monoamines [54].
267 At the intracellular border of TM3, the highly conserved Asp^{180}-Arg^{181}-Tyr^{182} motif is evident
268 for a strong ionic interaction with Glu^{430} residue adjacent to the intracellular end of TM6 that
269 plays a crucial role in GPCR signal transduction [55]. The sequence contains consensus Phe^{444}-
270 X-X-X-Trp^{448}-X-Pro^{450}-X-Phe^{452} motif in TM6 which is unique to biogenic monoamine GPCRs
271 [38]. Additionally, Se-HTR contains two potential post-translational palmitoylation cysteine
272 residues (Cys^{508} and Cys^{532}) [56] at the final intracellular region with a PDZ-domain binding
273 motif (Glu^{561}-Ser^{562}-Phe^{563}-Leu^{564}) at the C-terminus [57].

274 *Se-5HTR* is expressed in all developmental stages. It is expressed in immune-associated
275 tissues (hemocytes and fat body), digestive (gut) tissues, and nervous (brain) tissues at larval
276 stage. Three 5-HT receptors of *P. rapae* larvae are all expressed, although their expression levels
277 in tissues are different. Subtypes 1A and 1B receptor are highly expressed in nervous tissues
278 while subtype 7 receptor is mainly expressed in digestive tissue [36]. *Se-5HTR* was also highly
279 expressed in the gut like 5-HT_7 of *P. rapae*. Furthermore, our phylogenetic analysis of 5-HT
280 receptors showed that these two insect 5-HT_7s were closely related and clustered. Expression
281 levels of *Se-5HTR* in hemocytes were similar to those in the brain. This suggests that Se-5HTR is
282 associated with immune function as well as neurophysiological function. Indeed, bacterial or
283 fungal infection up-regulated the expression of *Se-5HTR*. The increase of *Se-5HTR* expression
284 might be explained by the up-regulation of *de novo* biosynthesis of its ligand, 5-HT, via increase

285 in expression of biosynthetic genes as seen in hemocytes of *P. rapae* larvae after immune
286 challenge [22].

287 The presence of 5-HT_7 receptor in hemocytes of *S. exigua* and its physiological function
288 associated with immune responses were supported by its sensitivity to specific 5-HTR inhibitors.
289 In response to 5-HT or bacterial challenge, *S. exigua* larvae exhibited significant increase of
290 THC. This up-regulation of THC was explained by mobilization of sessile hemocytes to
291 circulatory form by cytoskeletal rearrangement via a small G protein, Rac1 [45,52]. This
292 suggests that Se-5HTR can activate Rac1 to stimulate the hemocyte behavior. In vertebrates,
293 activation of 5-HT_7 receptor increases cAMP level via a trimeric G protein G_s and small G
294 proteins of Rho family including Cdc42, RhoA, and Rac1 via another trimeric G protein G_{12} [58].
295 This suggests that immune challenge can induce biosynthesis and release of 5-HT which then
296 binds to Se-5HTR on hemocytes and activates Rac1 to stimulate hemocyte behaviors. In addition,
297 the cAMP pathway triggered by Se-5HTR might activate Akt and ERK1/2 as seen in mammalian
298 cancer cells [59] to facilitate actin rearrangement to form cellular shape change of hemocytes.
299 These findings suggest that Se-5HTR plays a crucial role in hemocyte migration and cell shape
300 change during cellular immune responses. Indeed, RNAi of *Se-5HTR* expression resulted in
301 significant immunosuppression by exhibiting reduction in phagocytosis and nodulation.

302 Bacterial metabolites derived from two entomopathogens, *Xenorhabdus* and *Photorhabdus*,
303 inhibited cellular immune responses mediated by Se-5HTR. Especially, six chemical groups
304 (phenylethylamide, tryptamide, xenortide, xenocycloin, nematophin, and GameXPeptide) highly
305 inhibited both phagocytosis and nodulation, suggesting that they can inhibit Se-5HTR. This was
306 supported by their competitive inhibition with the ligand, 5-HT. Bacterial secondary metabolites
307 may be synthesized and released in the bacterium-nematode complex in order to defend immune

308 attack from target insect to compete with other microbes occurring in the insect cadaver and
309 facilitate host nematode development or bacterial quorum sensing [47]. It has been reported
310 phenylethylamides and tryptamides identified from *Xenorhabdus* can act as quorum quenching
311 activators by competitive binding to N-acylated homoserine lactone (AHL) receptor because
312 AHL accumulation drives gene expression of bioluminescence, virulence factor, and biofilm
313 formation in bacteria [60,61]. Xenortides are linear peptides consisting of 2-8 amino acids
314 synthesized from both *Xenorhabdus* and *Photorhabdus* [62]. They are synthesized in insect hosts
315 during infection with putative role in inhibiting prophenoloxidase activation to suppress insect
316 immunity [63]. Xenocycloins produced by *X. bovienii* are cytotoxic to hemocytes of *Galleria*
317 *melonella* [64]. Nematophin is synthesized by condensation of α-keto acid and tryptamine in *X.*
318 *nematophila.* It possesses a specific antibacterial activity against *Staphylococcus aureus* [65].
319 GameXPeptides are cyclic pentapeptides widely synthesized in both *Xenorhabdus* and
320 *Photorhabdus*. However, their biological functions remain unclear [66]. This current study
321 showed that these six compound classes could inhibit cellular immune responses by competitive
322 inhibition with 5-HT against Se-5HTR.

323 A novel phenylethylamide compound, PhX, was found to be highly inhibitory against Se-
324 5HTR. Derivatives of phenylethylamide compound (HB 4) exhibited different inhibitory
325 activities against cellular immune responses mediated by Se-5HTR. Especially, PhX containing
326 methoxy and hexahydropyrrolo[1,2-a]pyrazine-1,4-dione exhibited the highest inhibitory
327 activity. 5-HT receptors have been used for screening for potent insecticides with growth-
328 inhibiting or larvicidal activities against *Pseudaletia separata* [67]. Thus, PhX can be a candidate
329 for this application unless it shows mammalian or non-target species toxicity [68].

330

331 **Materials and methods**

332 **Insect rearing and microbial culture**

333 A laboratory strain of *S. exigua* was originated from Welsh onion field (Andong, Korea) and
334 maintained for ~20 years. Larvae of this laboratory strain were reared on an artificial diet [69] at
335 temperature of 25 ± 1°C and relative humidity of 60 ± 10% with a photoperiod of 16:8 h (L:D).
336 Under these conditions, larvae had five instars ('L1-L5'). Adults were reared with 10% sucrose
337 solution. For immune challenge, *Escherichia coli* Top10 (Invitrogen, Carlsbad, CA, USA) was
338 cultured in Luria-Bertani (LB) medium (BD Korea, Seoul, Korea) in a shaking incubator (200
339 rpm) at 37°C overnight (16 h).

340

341 **Chemicals**

342 Serotonin hydrochloride was purchased from Sigma-Aldrich Korea (Seoul, Korea). It was
343 dissolved in distilled water. SB-269970 (a specific inhibitor to 5-HT receptor subtype 7, 5-HT_7)
344 was purchased from Cayman Chemical Company (Korea). It was dissolved in desired
345 concentrations with dimethyl sulfoxide (DMSO). Fluorescein isothiocyanate (FITC) [2-(6-
346 hydroxy-3-oxo-3h-xanthen-9-yl)-5-isothiocyanatobenzoic acid] was purchased from Sigma-
347 Aldrich Korea. It was dissolved in DMSO to make a solution at 10 mg/mL. Anticoagulant buffer
348 (ACB) was prepared using 98 mM NaOH, 186 mM NaCl, 17 mM Na_2EDTA, and 41 mM citric
349 acid at pH 4.5. Phosphate-buffered saline (PBS) was prepared at pH 7.4 with 50 mM sodium
350 phosphate and 0.7% NaCl. Tris-buffered saline (TBS) was prepared using 150 mM NaCl, 50
351 mM Tris-HCl at pH 7.6. Hank's balanced salt solution (HBSS) was prepared with the following
352 compositions: 8 g NaCl, 400 mg KCl, 40 mg Na_2HPO_4, 60 mg KH_2PO_4, 1 g glucose, 140 mg
353 $CaCl_2$, 120 mg $MgSO_4$, and 350 mg $NaHCO_3$ in 1,000 mL distilled H_2O.

354

355 **Bioinformatics to search for 5-HT receptor and sequence analysis**

356 *S. exigua* 5-HT receptor (Se-5HTR) sequence was obtained from GenBank by manual annotation.
357 Briefly, a dopamine receptor sequence (AKR18180.1) of *Chilo suppressalis* was used to screen a
358 transcriptome (SRR1050532) of *S. exigua*. A blast contig (GARL01017386.1) was analyzed for
359 open reading frame (ORF) and the predicted amino acid sequence was used for analysis using
360 BlastP program against GenBank (www.ncbi.nlm.nih.gov). After confirming its high homologies
361 (E value < 10^{-20}) with other known insect 5HTRs, the resulting ORF sequence (= Se-5HTR) was
362 deposited at NCBI-GenBank (accession number: MH025798). Sequence alignment was
363 established using Clustal Omega tool (https://www.ebi.ac.uk/Tools/msa/clustalo/) provided by
364 European Bioinformatics Institution. Phylogenetic tree was generated with Neighbor-joining
365 method using Mega6 and ClustalW programs. Bootstrapping values were obtained with 1,000
366 repetitions to support branch and clustering. Protein domain was predicted using InterPro tool
367 (https://www.ebi.ac.uk/interpro/), pfam (http://pfam.xfam.org), and Prosite
368 (http://prosite.expasy.org/).

369

370 **RNA extraction and cDNA preparation**

371 Using Trizol reagent (Invitrogen), total RNAs were extracted from all developmental stages as
372 well as larval tissues (hemocyte, midgut, fat body, and brain) of *S. exigua* according to the
373 instruction of the manufacturer. Numbers of individuals used for RNA extraction for each
374 individual developmental stage were as follows: ~500 eggs, ~20 larvae for L1-L2, ~10 larvae for
375 L3, ~5 larvae for L4, one larva for L5, one pupa, and one adult. L5 larvae were used for RNA
376 extraction from different tissue samples. After extraction, total RNAs were resuspended in

377 nuclease-free water and cDNAs were synthesized from ~1 μg of RNAs using Maxime RT
378 Premix (Intron Biotechnology, Seoul, Korea) according to the manufacturer's instruction.
379
380 **Expression pattern of Se-5HTR by RT-qPCR**
381 A fragment of *Se-5HTR* was amplified with gene-specific primers (5'- CTT TAC CTT CGT
382 GTC TTC TC-3' and 5'- GGT GTC AGT CTT CTC ATT AC -3'). PCR was performed with 35
383 cycles of denaturation (94°C, 1 min), annealing (49°C, 1 min), and extension (72°C, 1 min). PCR
384 products were subjected to agarose gel electrophoresis to visually confirm their amplifications.
385 With the same gene-specific primers used in RT-PCR, RT-qPCR was performed in a qPCR
386 machine (CFX Connect™ Real-Time PCR Detection System, Bio-Rad, Hercules, CA, USA)
387 using SYBR Green Realtime PCR Master Mix (Toyobo, Osaka, Japan) under a guideline of
388 Bustin et al. [70]. The amplification used 40 cycles of 15 s at 95°C, 30 s at 60°C, and 45 s at
389 72°C. After PCR reactions, melting curves from 60 to 95°C were obtained to confirm unique
390 PCR products. A ribosomal protein, RL32, gene was used as a control with primers of 5'-ATG
391 CCC AAC ATT GGT TAC GG-3' and 5'-TTC GTT CTC CTG GCT GCG GA-3'. Each
392 treatment was independently triplicated. Relative quantitative analysis method ($2^{-\Delta\Delta CT}$) was used
393 to estimate mRNA expression levels of *Se-5HTR*.
394
395 **RNA interference (RNAi)**
396 Gene fragment of *Se-5HTR* was amplified from template DNA using gene-specific primers (5'-
397 CTT TAC CTT CGT GTC TTC TC-3' and 5'-GGT GTC AGT CTT CTC AT-3') possessing T7
398 RNA polymerase promoter sequence (5'-TAA TAC GAC TCA CTA TAG GGA GA-3') at 5'
399 ends. PCR was performed with 5 cycles of denaturation (94°C, 1 min), annealing (49°C, 1 min),

400 and extension (72°C, 1 min) followed by 30 cycles of denaturation (94°C, 1 min), annealing
401 (60°C, 1 min), and extension (72°C, 1 min) to synthesize DNA template for dsRNA synthesis.
402 Double-stranded RNA (dsRNA) against *Se-5HTR* ('dsSe-5HTR') was synthesized using
403 Megascript RNAi kit (Ambion, Austin, TX, USA) following the manufacturer's instruction. The
404 resulting dsRNA was blended with Metafectene PRO (Biontex, Plannegg, Germany) at 1:1 (v:v)
405 ratio and incubated at 25°C for 30 min for liposome formation. Two microliters of the prepared
406 mixture containing ~900 ng of dsRNA was injected twice into *S. exigua* larval hemocoel using a
407 microsyringe (Hamilton, Reno, NV, USA) equipped with a 26-gauge needle. The first injection
408 was at late L4 stage. It was repeated 12 h afterwards. RNAi efficacy at 0, 24, and 48 h post-
409 injection (PI) in reducing *Se-5HTR* expression was determined by RT-qPCR. At 24 h PI, treated
410 larvae were used for immune challenge experiments. Each treatment was replicated thrice using
411 10 larvae for each replication.
412
413 **Total hemocyte count (THC)**
414 Hemolymph was collected by cutting larval proleg and mixed with ACB (1:10, v/v). Hemocytes
415 were counted using a Neubauer hemocytometer (Superior Marienfeld, Lauda-Königshofen,
416 Germany) under a phase contrast microscope (BX41, Olympus, Tokyo, Japan) at 100×
417 magnification. Heat-killed (90°C, 30 min) *Escherichia coli* (5×10^5 cells/larva) and a test
418 chemical (5-HT or SB-269970) were co-injected into hemocoel through abdominal proleg of L5
419 larvae in a volume of 5 μL using a 10 μL micro-syringe (Hamilton) after surface-sterilization
420 with 70% ethanol. After 4 h of incubation at 25 ± 2°C, hemolymph of the insect was collected
421 and assessed for THC.
422

423 **Hemocyte-spreading analysis**

424 After hemolymph (~150 μL) was collected from five L5 larvae by cutting prolegs, it was mixed
425 with three times volume of ice-cold ACB and incubated on ice for 30 min. ACB-treated
426 hemolymph was then centrifuged at 800 × *g* for 5 min at 4°C. The resulting pellet was re-
427 suspended in 500 μL of filter-sterilized TC-100 insect cell culture medium (Welgene, Daegu,
428 Korea). On a glass coverslip placed in a moist chamber, 10 μL of hemocyte suspension was
429 applied and placed in a dark condition. Hemocytes were then fixed with 4% paraformaldehyde
430 (filter-sterilized) at 25°C for 10 min and then washed thrice with filter-sterilized PBS. Cells were
431 then permeabilized with 0.2% Triton-X dissolved in PBS at 25°C for 2 min and washed with
432 PBS. After that, hemocytes were blocked using 10% bovine serum albumin (BSA) dissolved in
433 PBS at 25°C for 10 min and washed again with PBS. Cells were then incubated with FITC-
434 tagged phalloidin in PBS for 60 min and washed thrice with PBS. Hemocytes nuclei were then
435 stained by incubating with 4′,6-diamidino-2-phenylindole (DAPI, 1 μg/mL) (Thermo Fisher
436 Scientific, Rockford, IL, USA) dissolved in PBS and washed thrice with PBS. Hemocytes were
437 then observed under a fluorescence microscope (DM2500, Leica, Wetzlar, Germany) at 400×
438 magnification. Hemocyte-spreading was dictated by appendages of F-actin outward the
439 hemocyte cell boundary.

440 To assess effect of *Se-5HTR* RNAi on hemocyte-spreading, hemocytes were collected at 24 h
441 after injecting dsSe-5HTR (~900 ng/larva). In separate experiments, 5-HT and 5-HTR inhibitor
442 SB-269970 were co-injected into dsRNA-treated larvae at ratios of 1:10 and 10:1 to check their
443 influence on hemocyte-spreading. At 6 h after co-injection, hemolymph was collected from the
444 treated larva and hemocyte-spreading was observed using the above-mentioned method.

445

446 **Nodulation assay**

447 Overnight culture of *E. coli* Top10 bacterial cells was washed with PBS and centrifuged at 1,120
448 × *g* for 10 min. L5 larvae were used to assess hemocyte nodule formation by immune-challenge
449 with bacterial injection (~1.8 × 10^5 cells/larva) through the abdominal proleg into larval
450 hemocoel using a microsyringe as previously described. To assess the effect of *Se-5HTR* RNAi
451 on nodule formation, bacterial challenge was performed at 24 h after injecting dsSe-5HTR (~900
452 ng/larva). To check the influence of chemicals on nodule formation, 2 μg of ketanserin and/or 10
453 μg of 5-HT was co-injected along with the bacterial suspension. In separate experiment, 1 μg of
454 the bacterial secondary metabolite was co-injected with the bacterial suspension to assess
455 immune suppression activity of the test compound. After an incubation period of 8 h at 25°C,
456 treated insects were dissected under a stereo microscope (SZX9, Olympus, Japan) to count
457 melanized nodule numbers. Each treatment was triplicated independently using five insects for
458 each replication.

459

460 **Phagocytosis assay**

461 Preparation of FITC-labeled bacterial cells followed the method described by Harlow and Lane
462 (1998). Briefly, *E. coli* Top10 cells were cultured in 50 mL of Luria-Bertani broth (37°C, 16 h).
463 These bacterial cells were then harvested by centrifuging 1 mL of the cultured broth at 1,120 × *g*
464 for 10 min at 4°C. Bacterial cells (10^5 cells/mL) were washed twice with TBS and re-suspended
465 in 1 mL of 0.1 M sodium bicarbonate buffer (pH 9.0). In the suspension, 1 μL of 10 mg/mL
466 FITC solution was added and immediately mixed. The mixture was then incubated under
467 darkness with end-over-end rotation at 25°C for 30 min. After the incubation, FITC-tagged
468 bacteria were harvested by centrifugation at 22,000 × *g* for 20 min at 4°C. These bacterial cells

469 were washed thrice with HBSS to remove unbound dye and re-suspended in TBS.

470 To assess *in vivo* phagocytosis activity, 5 μL of FITC-tagged *E. coli* suspension was injected
471 into the hemocoel of L5 larva through the proleg. To assess the effect of *Se-5HTR* RNAi on
472 phagocytosis activity, bacteria were injected at 24 h after injecting dsSe-5HTR (~900 ng/larva).
473 To check the influence of a specific 5-HT_7 receptor inhibitor on phagocytosis, 2 μg of SB-
474 269970 was co-injected with the tagged bacterial suspension. To determine the effect of
475 secondary metabolite on phagocytosis, 1 μg of bacterial secondary metabolite was co-injected
476 with tagged bacterial suspension. After 15 min of incubation, treated larvae were surface-
477 sterilized using 70% ethanol. With a pair of scissors, the proleg was cut to collect hemolymph
478 sample (~50 μL) in 150 μL of cold ACB with gentle shaking of the tube to mix hemolymph and
479 ACB thoroughly. Hemocyte monolayers were made using 50 μL of hemocyte suspension (~5 ×
480 10^3 cells) and left in a moist chamber for 15 min for hemocytes to settle and attach to the glass
481 surface. After the incubation period, monolayers were washed with TBS to remove plasma.
482 These monolayers were overlaid with 1% trypan blue dye solution to quench non-phagocytosed
483 bacterial cells. After 10 min, monolayers were washed again with TBS and then fixed with 1.5%
484 glutaraldehyde solution to observe under a fluorescence microscope at 400× magnification.
485 Hemocytes undergoing phagocytosis were counted from a total of 100 hemocytes observed from
486 different areas of each slide. Each observation was triplicated with three different slides.

487

488 **Preparation of organic extracts from bacterial culture broth**

489 *X. nematophila* K1 (Xn) and *P. temperate temperata* ANU101 (Ptt) bacteria were cultured in
490 TSB at 28°C for 48 h. Culture broths were centrifuged at 12,500 × *g* for 30 min and supernatants
491 were used for subsequent fractionation. To obtain ethyl acetate extract, the same volume (1 L) of

492 ethyl acetate was mixed with the supernatant and separated into organic and aqueous fractions.
493 Ethyl acetate extract ('EAX') was dried using a rotary evaporator (Sunil Eyela, Seongnam,
494 Korea) at 40°C. The resulting extract (0.2 mg) was obtained from 1 L cultured broth and
495 resuspended with 5 mL of methanol. The aqueous phase was then combined with 1 L of butanol.
496 Butanol extract ('BX') was also dried using the rotary evaporator at 40°C and the resulting
497 extract (0.2 mg) was resuspended with 5 mL of methanol.
498

499 **Secondary bacterial metabolites – biological activity against immune responses**

500 Secondary metabolites (37 samples, S4 Fig) derived from *Xenorhabdus* and *Photorhabdus*
501 cultures were from the Bode lab compound collection named 'HB' compounds. Their biological
502 activities for suppressing *S. exigua* immunity were then determined. Individual chemicals were
503 dissolved in DMSO, diluted into desired concentrations with DMSO, and stored at -20°C.
504 For hemocyte nodulation inhibition assay, overnight culture of *E. coli* bacterial cells was
505 washed with PBS. Test compound (1 μg/larva) was injected into larval hemocoel along with the
506 bacterial suspension (~1.8×10^5 cfu/larva) using a microsyringe as previously described. Insects
507 were then incubated at 25°C for 8 h. After the incubation period, insects were dissected and
508 nodule numbers were counted as described above. Each treatment was triplicated independently
509 using five insects for each replication. For phagocytosis inhibition assay, 5 μL of FITC-tagged *E.*
510 *coli* suspension along with 1 μg of test compound was injected into L5 larval hemocoel. After 15
511 min of incubation period, hemocytes undergoing phagocytosis were counted as previously
512 described.
513

514 **Secondary bacterial metabolites – competitive assay with 5-HT**

515 To determine effects of bacterial secondary metabolites on nodulation and phagocytosis, 10
516 potent chemicals were selected based on their common inhibitory activity on both phagocytosis
517 and nodulation and their median inhibition concentration (IC_{50}) values were calculated.
518 Percentages of phagocytosis against increasing concentrations of HB chemicals were calculated
519 and their IC_{50} values were calculated using Probit analysis
520 (https://probitanalysis.wordpress.com). To assess a competitive inhibitory activity between test
521 compound and 5-HT, HB chemicals were injected in different doses (0, 0.01, 0.1, 1 and 10
522 μg/larva) along with a fixed 5-HT concentration (1 μg/larva) and FITC-tagged bacteria (500
523 cells/larva). In a separate experiment, different doses of 5-HT were injected into the larvae with a
524 fixed HB compound content (1 μg/larva). At 15 min after bacterial injection, hemocytes from
525 treated larvae were collected in ACB and phagocytosis assay was performed as described above.
526

527 **Chemical derivatives and their inhibitory activities against Se-5HTR**

528 Based on potent phenylethylamide (PEA) HB compounds, 45 additional PEA samples (S5 Fig)
529 were obtained from Korea Chemical Bank of the Korea Research Institute of Chemical
530 Technology (KRICT). Derivative compounds were dissolved in DMSO, diluted into desired
531 concentrations with DMSO, and stored at -20°C. These PEA chemicals were then tested for their
532 abilities to suppress nodule formation and phagocytosis in *S. exigua* as described above. For
533 nodulation inhibition assay, each chemical (150 ng/larva) was injected into larval hemocoel
534 along with bacterial suspension (~1.8×10^5 cfu/larva). Each treatment was triplicated
535 independently using five insects for each replication. For phagocytosis inhibition assay, 5 μL of
536 FITC-tagged *E. coli* suspension along with 150 ng of each chemical was injected into L5 larval

hemocoel of *S. exigua*. After incubating for 15 min, hemocytes undergoing phagocytosis were counted using previously described method.

Chemical synthesis of PhX

A potent chemical was designed as PhX ((*S*)-2-(1,4-dioxohexahydropyrrolo[1,2-*a*]pyrazin-2(*1H*)-yl)-*N*-(4-methoxyphenethyl)acetamide) and chemically synthesized according to a method described in S6 Fig.

Statistical analysis

All studies were triplicated independently. Results are expressed as mean ± standard error. Results were plotted using Sigma plot (Systat Software, San Jose, CA, USA). Means were compared by least squared difference (LSD) test of one-way analysis of variance (ANOVA) using POC GLM of SAS program [71] and discriminated at Type I error = 0.05.

Funding

This work was supported by a grant (No. 2017R1A2133009815) of the National Research Foundation (NRF) funded by the Ministry of Science, ICT and Future Planning, Republic of Korea. This work was also supported by a project (No SI1808, Development of crop protection agents leading the future market). The chemical library used in this research was provided by Korea Chemical Bank (http://www.chembank.org) of the Korea Research Institute of Chemical Technology (KRICT).

Acknowledgments

We appreciate Youngim Song for ordering and arranging materials and Malsook Cho for rearing insects. Work in the Bode lab was supported by the LOEWE Center Translational Biodiversity Genomics funded by the state of Hesse, Germany.

Author Contributions

Conceptualization: Yonggyun Kim.

Formal analysis: Ariful Hasan, Yonggyun Kim.

Investigation: Hyun-Suk Yeom, Jaewook Ryu, Helge B. Bode, Yonggyun Kim.

Project administration: Yonggyun Kim.

Supervision: Hyun-Suk Yeom, Jaewook Ryu, Helge B. Bode, Yonggyun Kim.

Writing – original draft: Ariful Hasan, Yonggyun Kim.

Writing – review & editing: Ariful Hasan, Hyun-Suk Yeom, Jaewook Ryu, Helge B. Bode, Yonggyun Kim.

574 **References**

575

576 1. Roshchina VV. 2010. New trends and perspectives in the evolution of neurotransmitters in
577 microbial, plant, and animal cells. Adv Exp Med Biol. 2016;874:25-77.
578 2. Lovenberg W, Weissbach H, Udenfriend S. 1962. Aromatic L-amino acid decarboxylase. J
579 Biol Chem. 1962;237:89-93.
580 3. Hufton SE, Jennings IG, Cotton RG. Structure and function of the aromatic amino acid
581 hydroxylases. Biochem. J. 1995;311:353-66.
582 4. Roberts KM, Fitzpatrick PF. 2013. Mechanisms of tryptophan and tyrosine hydroxylase.
583 IUBMB Life 2013;65:350-357.
584 5. Zhang X, Beaulieu JM, Sotnikova TD, Gainetdinov RR, Caron MG. Tryptophan
585 hydroxylase-2 controls brain serotonin synthesis. Science. 2004;305:217.
586 6. Gershon MD, Tack J. The serotonin signaling system: from basic understanding to drug
587 development for functional GI disorders. Gastroenterology. 2007;132:397-414.
588 7. Richtand NM, McNamara RK. Serotonin and dopamine interactions in psychosis prevention.
589 Prog Brain Res. 2008;172:141-53.
590 8. Monti JM. Serotonin control of sleep-wake behavior. Sleep Med Rev. 2011;15:269-81.
591 9. Švob Štrac D, Pivac N, Mück-Šeler D. The serotonergic system and cognitive function.
592 Transl Neurosci. 2016;7:35-49.
593 10. Seuwen K, Pouysségur J. Serotonin as a growth factor. Biochem. Pharmacol. 1990;39:985-
594 90.
595 11. Li N, Wallén NH, Ladjevardi M, Hjemdahl P. Effects of serotonin on platelet activation in
596 whole blood. Blood Coagul Fibrinolysis 1997;8:517-23.

597 12. Hayashi K, Fujita Y, Ashizawa T, Suzuki F, Nagamura Y, Hayano-Saito Y. Serotonin
598 attenuates biotic stress and leads to lesion browning caused by a hypersensitive response to
599 *Magnaporthe oryzae* penetration in rice. Plant J. 2016;85:46-56.
600 13. Majeed ZR, Abdeljaber E, Soveland R, Cornwell K, Bankemper A, Koch F, et al.
601 Modulatory action by the serotonergic system: behavior and neurophysiology in *Drosophila*
602 *melanogaster*. Neural Plast. 2016;2016:1-23.
603 14. Huser A, Eschment M, Güllü N, Kan C, Böpple K, Pankevych L. et al. Anatomy and
604 behavioral function of serotonin receptors in *Drosophila melanogaster* larvae. PLoS One
605 2017;12:e0181865.
606 15. Becnel J, Johnson O, Luo J, Nässel DR, Nichols CD. The serotonin 5-HT_{7Dro} receptor is
607 expressed in the brain of *Drosophila*, and is essential for normal courtship and mating. PLoS
608 One 2011;6:e20800.
609 16. Yuan Q, Lin F, Zheng X, Sehgal A. Serotonin modulates circadian entrainment in
610 *Drosophila*. Neuron. 2005;47:115-27.
611 17. Nichols CD. 5-HT_2 receptors in *Drosophila* are expressed in the brain and modulate aspects
612 of circadian behaviors. Dev Neurobiol. 2007;67:752-63.
613 18. Yuan Q, Joiner WJ, Sehgal A. A sleep-promoting role for the *Drosophila* serotonin receptor
614 1A. Curr. Biol. 2006;16:1051-62.
615 19. Neckameyer WS, Coleman CM, Eadie S, Goodwin SF. Compartmentalization of neuronal
616 and peripheral serotonin synthesis in *Drosophila melanogaster*. Genes Brain Behav.
617 2007;6:756-69.
618 20. Dierick HA, Greenspan RJ. Serotonin and neuropeptide F have opposite modulatory effects
619 on fly aggression. Nat. Genet. 2007;39:678-82.

620 21. Kaplan DD, Zimmermann G, Suyama K, Meyer T, Scott MP. A nucleostemin family
621 GTPase, NS3, acts in serotonergic neurons to regulate insulin signaling and control body
622 size. Genes Dev. 2008;22:1877-93.
623 22. Qi YX, Huang J, Li MQ, Wu YS, Xia RY, Ye GY. Serotonin modulates insect hemocyte
624 phagocytosis via two different serotonin receptors. Elife 2016;5:e12241.
625 23. Python F, Stocker RF. Immunoreactivity against choline acetyltransferase, gamma-
626 aminobutyric acid, histamine, octopamine, and serotonin in the larval chemosensory system
627 of *Drosophila melanogaster*. J. Comp. Neurol. 2002;453:157-67.
628 24. Dasari S, Cooper RL. Direct influence of serotonin on the larval heart of *Drosophila*
629 *melanogaster*. J. Comp. Physiol. B 2006;176:349-57.
630 25. Rodriguez MVG, Campos AR. Role of serotonergic neurons in the *Drosophila* larval
631 response to light. BMC Neurosci. 2009;10:66.
632 26. Barnes, N.M., Sharp, T., 1999. A review of central 5-HT receptors and their function.
633 Neuropharmacology 38, 1083-1152.
634 27. Nichols DE, Nichols CD. Serotonin receptors. Chem Rev. 2008;108:1614-41.
635 28. Roth BL. The serotonin receptors : from molecular pharmacology to human therapeutics.
636 Humana Press, Totowa, New Jersey. 2006.
637 29. Thompson AJ, Lummis SCR. 5-HT_3 Receptors. Curr. Pharm. Des. 2006;12:3615-30.
638 30. Watanabe T, Sadamoto H, Aonuma H. Identification and expression analysis of the genes
639 involved in serotonin biosynthesis and transduction in the field cricket *Gryllus bimaculatus*.
640 Insect Mol Biol. 2011;20:619-35.
641 31. Ono H, Yoshikawa H. Identification of amine receptors from a swallowtail butterfly, *Papilio*
642 *xuthus* L.: cloning and mRNA localization in foreleg chemosensory organ for recognition of

643 host plants. Insect Biochem Mol Biol. 2004;34:1247-56.

644 32. Vleugels R, Lenaerts C, Baumann A, Vanden BJ, Verlinden H. Pharmacological
645 characterization of a 5-HT_1-type serotonin receptor in the red flour beetle, *Tribolium*
646 *castaneum*. PLoS One 2013;8:e65052.

647 33. Troppmann B, Balfanz S, Baumann A, Blenau W. Inverse agonist and neutral antagonist
648 actions of synthetic compounds at an insect 5-HT_1 receptor. Br. J. Pharmacol.
649 2010;159:1450-62.

650 34. Guo X, Ma Z, Kang L. Serotonin enhances solitariness in phase transition of the migratory
651 locust. Front. Behav Neurosci. 2013;7:129.

652 35. Qi YX, Xia RY, Wu YS, Stanley D, Huang J, Ye GY. Larvae of the small white butterfly,
653 *Pieris rapae*, express a novel serotonin receptor. J Neurochem. 2014;131:767-77.

654 36. Qi YX, Jin M, Ni XY, Ye GY, Lee Y, Huang J. Characterization of three serotonin receptors
655 from the small white butterfly, *Pieris rapae*. Insect Biochem. Mol. Biol. 2017;87:107-16.

656 37. Thamm M, Balfanz S, Scheiner R, Baumann A, Blenau W. Characterization of the 5-HT_{1A}
657 receptor of the honeybee (*Apis mellifera*) and involvement of serotonin in phototactic
658 behavior. Cell Mol. Life Sci. 2010;67:2467-79.

659 38. Schlenstedt J, Balfanz S, Baumann A, Blenau W. Am5-HT_7: molecular and pharmacological
660 characterization of the first serotonin receptor of the honeybee (*Apis mellifera*). J
661 Neurochem. 2006;98:1985-98.

662 39. Berridge MJ, Patel N. Insect salivary glands - stimulation of fluid secretion by 5-
663 hydroxytryptamine and adenosine-3', 5'-monophosphate. Science. 1968;162:462-3.

664 40. Berridge MJ. The role of 5-hydroxytryptamine and cyclic AMP in the control of fluid
665 secretion by isolated salivary glands. J Exp Biol. 1970;53:171-86.

666 41. Vanhoenacker P, Haegeman G, Leysen JE. 5-HT_7 receptors: current knowledge and future
667 prospects. Trends Pharmacol. Sci. 2000;21:70-7.
668 42. Molaei G, Lange AB. The association of serotonin with the alimentary canal of the African
669 migratory locust, *Locusta migratoria*: distribution, physiology and pharmacological profile.
670 J Insect Physiol. 2003;49:1073-182.
671 43. Baines D, DeSantis T, Downer RGH. Octopamine and 5-hydroxytryptamine enhance the
672 phagocytic and nodule formation activities of cockroach (*Periplaneta americana*)
673 haemocytes. J Insect Physiol. 1992;38:905-14.
674 44. Kim K, Madanagapol N, Lee D, Ki Y. Octopamine and 5-hydroxytryptamine mediate
675 hemocytic phagocytosis and nodule formation via eicosanoids in the beet armyworm,
676 *Spodoptera exigua*. Arch. Insect Biochem. Physiol. 2009;90:162-76.
677 45. Kim GS, Kim Y. Up-regulation of circulating hemocyte population in response to bacterial
678 challenge is mediated by octopamine and 5-hydroxytryptamine via Rac1 signal in
679 *Spodoptera exigua*. J. Insect Physiol. 2010;56:559-66.
680 46. Kim Y, Ji D, Cho S, Park Y. Two groups of entomopathogenic bacteria, *Photorhabdus* and
681 *Xenorhabdus*, share an inhibitory action against phospholipase A_2 to induce host
682 immunodepression. J Invertebr Pathol. 2005;89: 258-64.
683 47. Shi YM, Bode HB. Chemical language and warfare of bacterial natural products in bacteria-
684 nematode-insect interactions. Nat Prod Rep 2018;35:309-35.
685 48. Tobias NJ, Shi YM, Bode HB. Refining the natural product repertoire in entomopathogenic
686 bacteria. Trends Microbiol. 2018;26:833-40.
687 49. Barak LS, Tiberi M, Freedman NJ, Kwatra MM, Lefkowitz RJ, Caron MG. A highly
688 conserved tyrosine residue in G protein-coupled receptors is required for agonist-mediated

689 ß2-adrenergic receptor sequestration. J Biol Chem 1994;269:2790-5.

690 50. Ji TH, Grossmann M, Ji I. G protein-coupled receptors. I. Diversity of receptor-ligand
691 interactions. J Biol Chem. 1998;273:17299-302.

692 51. Huang ES. Construction of a sequence motif characteristic of aminergic G protein-coupled
693 receptors. Protein Sci. 2003;12:1360-67.

694 52. Park J, Stanley D, Kim Y. Rac1 mediates cytokine-stimulated hemocyte spreading via
695 prostaglandin biosynthesis in the beet armyworm, *Spodoptera exigua*. J Insect Physiol.
696 2013;59:682-9.

697 53. Venkatakrishnan AJ, Deupi X, Lebon G, Tate CG, Schertler GF, Babu MM. Molecular
698 signatures of G-protein-coupled receptors. Nature 2013;494:185-94.

699 54. Ho BY, Karschin A, Branchek T, Davidson N, Lester HA. The role of conserved aspartate
700 and serine residues in ligand binding and in function of the 5-HT_{1A} receptor: A site-directed
701 mutation study. FEBS Lett. 1992;312:259-62.

702 55. Shapiro DA, Kristiansen K, Weiner DM, Kroeze WK, Roth BL. Evidence for a model of
703 agonist-induced activation of 5-hydroxytryptamine 2A serotonin receptors that involves the
704 disruption of a strong ionic interaction between helices 3 and 6. J. Biol. Chem.
705 2002;277:11441-9.

706 56. Qanbar R, Bouvier M. Role of palmitoylation/depalmitoylation reactions in G-protein-
707 coupled receptor function. Pharmacol. Ther. 2003;97:1-33.

708 57. Romero G, von Zastrow M, Friedman PA. Role of PDZ proteins in regulating trafficking,
709 signaling, and function of GPCRs: means, motif, and opportunity. Adv Pharmacol.
710 2011;62:279-314.

711 58. Guseva D, Wirth A, Ponimaskin E. Cellular mechanisms of the 5-HT_7 receptor-mediated

712 signaling. Front. Behav. Neurosci. 2014;8:306.
713 59. Choi C, Helfman DM. The Ras-ERK pathway modulates cytoskeleton organization, cell
714 motility and lung metastasis signature genes in MDA-MB-231 LM2. Oncogene
715 2014;33:3668-76.
716 60. Papenfort K, Bassler BL. Quorum sensing signal-response systems in Gram-negative
717 bacteria. Nat. Rev. Microbiol. 2016;14:576-88.
718 61. Bode E, He Y, Vo TD, Schultz R, Kaiser M, Bode HB. Biosynthesis and function of simple
719 amides in *Xenorhabdus doucetiae*. Environ. Microbiol. 2017;19:4564-75.
720 62. Reimer D, Nollmann FI, Schultz K, Kaiser M, Bode HB. Xenortide biosynthesis by
721 entomopathogenic *Xenorhabdus nematophila*. J Nat Prod. 2014;77:1976-80.
722 63. Bloudoff K, Schmeing TM. Structural and functional aspects of the nonribosomal peptide
723 synthetase condensation domain superfamily: discovery, dissection and diversity. Biochim
724 Biophys Acta 2017;1865:1587-604.
725 64. Proschak A, Zhou Q, Schöner T, Thanwisai A, Kresovic D, Dowling A, et al. Biosynthesis of
726 the insecticidal xenocyloins in *Xenorhabdus bovienii*. Chembiochem. 2014;15:369-72.
727 65. Li J, Chen G, Webster JM. Nematophin, a novel antimicrobial substance produced by
728 *Xenorhabdus nematophilus* (Enterobactereaceae). Can J Microbiol. 1997;43:770-3.
729 66. Nollmann FI, Dauth C, Mulley G, Kegler C, Kaiser M, Waterfield NR. et al. Insect-specific
730 production of new GameXPeptides in *Photorhabdus luminescens* TTO1, widespread natural
731 products in entomopathogenic bacteria. Chembiochem. 2015;16:205-8.
732 67. Cai M, Li Z, Fan F, Huang Q, Shao X, Song G. Design and synthesis of novel insecticides
733 based on the serotonergic ligand 1-[(4-Aminophenyl) ethyl]-4-[3-(trifluoromethyl) phenyl]
734 piperazine (PAPP). J Agric Food Chem. 2009;58:2624-9.

735 68. Verlinden H, Vleugels R, Broeck JV. Serotonin, serotonin receptors and their actions in
736 insects. Neurotransmitter. 2015;2:e314
737 69. Shrestha S, Stanley D, Kim Y. PGE_2 induces oenocytoid cell lysis via a G protein-coupled
738 receptor in the beet armyworm, *Spodoptera exigua*. J. Insect Physiol. 2011; 57:1568-76.
739 70. Bustin SA, Benes V, Garson JA, Hellemans J, Huggett J, Kubista M, et al. The MIQE
740 guidelines: minimum information for publication of quantitative real-time PCR experiments.
741 Clin. Chem. 2009;55:4.
742 71. SAS Institute. SAS/STAT user's guide. SAS Institute, Inc., Cary, NC. 1989.

743 **Figure captions**

744

745 **Fig. 1. Bioinformatics analysis of a novel 5-HTR$_7$ identified from *S. exigua* (Se-5HTR:**
746 **MH025798). (A)** Phylogenetic analysis of 5HTRs. Amino acid sequences were retrieved from
747 GenBank: Hs5HTR1D (NP_000855.1), Ss5HTR1D (NP_999323.1), Rn5HTR1D
748 (NP_036984.1), Oc5HTR1D (NP_001164624.1), NP_000854.1 Hs5HTR1B (NP_000854.1),
749 Dr5HTR1D (NP_001139158.1), Hs5HTR1F (NP_000857.1), Hs5HTR1E (NP_000856.1),
750 Cp5HTR1E (NP_001166222.1), Hs5HTR1A (NP_000515.2), Ap5HTR1B (ABY85411.1),
751 Ms5HTR (ABI33827.1), Pr5HTR1B (XP_022120028.1), Am5HTR1 (NP_001164579.1),
752 Dm5HTR1B (NP_001163201.2), Pa5HTR1 (CAX65666.1), Pr5HTR1A (XP_022129638.1),
753 Ap5HTR1A (ABY85410.1), Hs5HTR7 (P34969), Rn5HTR7 (P32305), Pr5HTR7
754 (AMQ67549.1), Am5HTR7 (NP_001071289.1), Dm5HTR7 (NP_524599.1), Ae5HTR7
755 (Q9GQ54), Hs5HTR4 (Q13639), Cp5HTR4 (O70528), Rn5HTR4 (Q62758), Mm5HTR4
756 (P97288), Hs5HTR6 (P50406), Pt5HTR6 (Q5IS65), It5HTR6 (XP_005317590.1), Rn5HTR6
757 (P31388), Mm5HTR6 (Q9R1C8), Cp5HTR6 (XP_003471412.1), Pm5HTR2A (KPJ17794.1),
758 Pr5HTR2A (XP_022112310.1), Bm5HTR2A (NP_001296483.1), Cl5HTR2A
759 (XP_014254278.1), Rp5HTr2B (AKQ13312.1), Mq5HTR2A (KOX78271.1), Am5HTr2B
760 (NP_001189389.1), Hs5HTR2A (NP_000612.1), Hs5HTR2C (NP_000859.1), Hs5HTR2B
761 (NP_000858.3), Pt5HTR2C (XP_015921531.1), Mp5HTR2C (XP_022169104.1), Am5HTr2A
762 (NP_001191178.1), Pr5HTR2C (XP_022122944.1), Ba5HTR2C (XP_023955125.1),
763 Rn5HTR5B (P35365), Mm5HTR5B (P31387), Hs5HTR5A (NP_076917.1), Rn5HTR5A
764 (P35364), Mm5HTR5A (P30966), Hs5HTR3C (NP_570126.2), Hs5HTR3E (NP_001243542.1),
765 Hs5HTR3D (NP_001157118.1), Hs5HTR3B (NP_006019.1), Rn5HTR3B (NP_071525.1),

766 Hs5HTR3A (AP35868.1), Cp5HTR3A (O70212), Rn5HTR3A (NP_077370.2), Mm5HTR3A
767 (P23979). The phylogenetic tree was constructed using neighbor-joining method. Bootstrap
768 values on branch nodes were obtained after 1,000 repetitions. **(B)** Amino acid sequence
769 alignment of Se-5HTR with orthologous receptors from *Homo sapiens* (Hs-5HTR7: P34969),
770 *Drosophila melanogaster* (Dm-5HTR7: NP_524599.1), *Manduca sexta* (Ms-5HTR7:
771 AGL46976.1), and *Pieris rapae* (Pr-5HTR7: AMQ67549.1). Identical residues among these five
772 sequences are illustrated as white letters against black. Dashes within sequences indicate gaps
773 introduced to maximize homology. Putative seven transmembrane domains (TM1-TM7) are
774 shown as blue bars. Potential N-glycosylation sites ( ), potential phosphorylation sites for
775 protein kinase A and/or C ( ), potential residue to interacts with 5-HT amino group ( ) and 5-
776 HT hydroxyl group ( ), potential disulfide bond groups ( ), and potential post translational
777 palmitoylation sites ( ) are indicated. Overbars indicate unique motif to aminergic receptor,
778 agonist mediated sequestration and resensitization motif, and PDZ-domain binding motif,
779 respectively. Conserved domains were determined using InterPro tool
780 (https://www.ebi.ac.uk/interpro/) and Prosite (http://prosite.expasy.org/) whereas other residues
781 and motifs were predicted using several tools from DTU bioinformatics
782 (www.cbs.dtu.dk/services/).
783
784 **Fig. 2. Expression profile of *Se-5HTR*. (A)** Differential expression of *Se-5HTR* in different
785 developmental stages: egg, larval instars ('L1-L5'), pupa ('Pu'), and adult ('Ad'). **(B)**
786 Differential expression of *Se-5HTR* in different tissues of L5 larvae: hemocyte ('HC), midgut
787 ('GUT'), fat body ('FB'), and brain ('BR'). **(C)** Expression pattern of *Se-5HTR* in immune-
788 challenged L5 larvae: *Escherichia coli* ('Ec'), *Xenorhabdus nematophila* ('Xn'), *Photorhabdus*

789 *temperata temperata* ('Ptt'), *Serratia marcescens* ('Sm'), and *Beauveria bassiana* ('Bb').
790 Immune challenge was performed by injecting each L5 larva with 1.8×10^5 cells of bacteria or 5
791 $\times 10^5$ conidia of fungi. After incubation at 25°C for 8 h, gene expression analysis was performed
792 using RT-PCR and RT-qPCR. As a constitutive expressional control, a ribosomal gene, *RL32*,
793 was used for expression analysis in RT-PCR and RT-qPCR. Each measurement was replicated
794 three times with independent biological samples. Histogram bars annotated with the same letter
795 are not significantly different at Type I error = 0.05 (LSD test).
796
797 **Fig. 3. Effect of an inhibitor specific to 5-HT$_7$ receptor ('SB-269970') on hemocyte**
798 **behaviors of *S. exigua*. (A)** Total hemocyte count (THC) analysis in L5 larvae. For the assay, 2
799 μg of 5-HT or 2 μg of SB-269970 was injected. THC was assessed with or without bacterial co-
800 injection (1.8×10^5 cells per larva). **(B)** Hemocyte-spreading behavior analysis. Hemocyte-
801 spreading was assessed with a 20 μL reaction mixture containing 1 or 2 μL test chemical with 18
802 or 19 μL hemocytes. 5-HT was co-applied with SB-269970 at ratios of 1:10 (2 μg 5-HT: 20 μg
803 SB-269970) and 10:1 (20 μg 5-HT: 2 μg SB-269970). Spread cells were stained with F-actin and
804 FITC-labeled phalloidin. Nuclei were stained with DAPI. Each treatment was independently
805 replicated three times. Histogram bars indicate percentages of spread hemocytes and error bars
806 indicate standard deviation. Histogram bars annotated with the same letter are not significantly
807 different at Type I error = 0.05 (LSD test).
808
809 **Fig. 4. RNA interference (RNAi) of *Se-5HTR* and suppression of hemocyte behaviors. (A)**
810 RNAi of *Se-5HTR* expression with a gene-specific dsRNA (dsSe-5HTR). About 900 ng of dsSe-
811 5HTR was injected to L5. At 0, 12, 24, and 48 h post-injection (PI), expression levels of *Se-*

812 *5HTR* were assessed from whole body. Expression levels of *Se-5HTR* in different tissue parts
813 were assessed at 24 h PI. As a constitutive expressional control, a ribosomal gene, *RL32*, was
814 used for expression analysis in RT-PCR and RT-qPCR. As a control RNAi (dsCON), dsRNA
815 specific to *CpBV-ORF302* (a viral gene) was used for expression analysis. In RT-qPCR, each
816 treatment was triplicated. **(B)** Influence of RNAi on up-regulation of total hemocyte count (THC)
817 in response to bacterial challenge. At 24 h PI of dsSe-5HTR, hemolymph was collected from L5
818 larvae for THC assessment. Each treatment was replicated three times. **(C)** Influence of RNAi on
819 hemocyte-spreading behavior. For spreading assay, hemocytes from larvae treated with dsRNA
820 were collected at 24 h. Each treatment was independently replicated three times. Spread cells
821 were stained with F-actin and FITC-labeled phalloidin. Nuclei were stained with DAPI.
822 Histogram bars indicate percentages of spread hemocytes and error bars indicate standard
823 deviation. Different letters above standard error bars indicate significant difference among means
824 at type I error = 0.05 (LSD test). Asterisks represent significant difference between control and
825 treatment in each tissue.
826
827 **Fig. 5. RNA interference (RNAi) of *Se-5HTR* and suppression of cellular immune responses.**
828 **(A)** Analysis of phagocytosis in L5 larvae of *S. exigua*. FITC-tagged *E. coli* were injected into
829 L5 larvae at 24 h post-injection of dsSe-5HTR. A specific inhibitor (SB-269970) to 5-HT_7
830 receptor was co-injected at a dose of 2 μg along with FITC-tagged bacteria. At 15 min after
831 injection, phagocytic cells were observed under a fluorescent microscope at 400 × magnification
832 and percentage of phagocytotic hemocytes was calculated from randomly chosen 100 cells. Total
833 hemocytes were observed from bright-field ('BF'). Each treatment was independently replicated
834 three times. **(B)** Nodulation assay. After RNAi, *E. coli* (1.8×10^5 cells/larva) was injected to L5

835 larvae. SB-269970 (2 μg/larva) was co-injected with bacteria. After 8 h incubation at 25°C,
836 treated insects were assessed for nodule formation. Histogram bars indicate percentages of
837 phagocytosis and error bars indicate standard deviation. Histogram bars annotated with the same
838 letter are not significantly different at Type I error = 0.05 (LSD test).
839
840 **Fig. 6. Immunosuppressive activities of organic extracts from culture broth of**
841 ***Xenorhabdus nematophila* ('Xn') and *Photorhabdus temperata temperata* ('Ptt') bacteria**
842 **against L5 larvae of *S. exigua*.** Each larva was injected with *E. coli* (10^5 cells) along with 1 μL
843 of ethyl acetate ('EAX') or butanol ('BX') extract. **(A)** Phagocytosis in L5 larvae. FITC-tagged
844 *E. coli* were injected to L5 larvae at 24 h post-injection of an organic extract. After 15 min,
845 phagocytic cells were observed under a fluorescent microscope at 400 × magnification and
846 percentage of phagocytotic hemocytes was calculated from randomly chosen 100 cells. Each
847 treatment was independently replicated three times. **(B)** Nodule formation. *E. coli* (1.8×10^5
848 cells/larva) was injected to L5 larvae. An organic extract was co-injected with the bacteria. After
849 8 h of incubation at 25°C, treated insects were assessed for nodule formation. Each treatment
850 was replicated with 10 larvae. Different letters above standard deviation bars indicate significant
851 difference among means at Type I error = 0.05 (LSD test).
852
853 **Fig. 7. Screening 37 bacterial secondary metabolites derived from *X. nematophila* and *P.***
854 ***temperata temperata* for their effects on cellular immune responses mediated by Se-5HTR in**
855 ***S. exigua*. (A)** Screening with phagocytosis assay. FITC-tagged *E. coli* cells were injected to L5
856 larvae along with 1 μg of each test chemical. After 15 min, phagocytic cells were observed under
857 a fluorescent microscope at 400 × magnification and percentage of phagocytotic hemocytes was

858 calculated from randomly chosen 100 cells. Each treatment was independently replicated three
859 times. **(B)** Screening with nodule formation assay. *E. coli* (1.8×10^5 cells/larva) was injected to
860 L5 larvae along with 1 μg of each test chemical. After 8 h of incubation at 25°C, treated insects
861 were assessed for nodule formation. Each treatment was replicated with 10 larvae. Asterisks
862 above standard deviation bars indicate significant difference compared to control ('CON'
863 without inhibitor) at Type I error = 0.05 (*), 0.01 (**), and 0.005 (***) (LSD test).
864

865 **Fig. 8. Competitive inhibition of 10 selected bacterial metabolites derived from *X.***
866 ***nematophila* and *P. temperata temperata* with 5-HT against Se-5HTR mediating**
867 **phagocytosis.** FITC-tagged *E. coli* cells were injected to L5 larvae along with test chemicals.
868 After 15 min, phagocytic cells were observed under a fluorescent microscope at 400 ×
869 magnification and percentage of phagocytotic hemocytes was calculated from randomly chosen
870 100 cells. Each treatment was independently replicated three times. **(A)** Dose-response of
871 inhibitory compound (0, 0.01, 0.1, 1, and 10 μg/larva) with a fixed 5-HT concentration (1
872 μg/larva). **(B)** Dose-response of 5-HT (0, 0.02, 0.2, 2 and 20 μg/larva) with a fixed HB
873 compound concentration (1 μg/larva). 'CON' represents a positive control without any inhibitor.

874

875 **Fig. 9. Validation of phenylethylamide (PEA) compounds for their inhibitory activities**
876 **against 5-HTR using derivatives with different side chains ('X' and 'Y' of PEA skeleton).**
877 **(A)** Screening of 45 PEA derivatives for their effects on hemocyte phagocytosis of *S. exigua*
878 with HB 44, a potent bacterial metabolite, as reference. PEA compounds (300 ng/larva) were
879 injected into hemocoels of L5 larvae along with FITC-tagged bacteria. After incubating for 15
880 min, hemocytes were assessed for phagocytosis. Asterisks above standard deviation bars indicate

881 significant difference compared to control ('CON' without inhibitor) at Type I error = 0.05 (*),
882 0.01 (**), and 0.005 (***) (LSD test). **(B)** Chemical structures of three selected PEA compounds
883 and their median inhibitory doses (IC_{50}). **(C)** Competitive inhibition of the three selected PEA
884 derivatives with 5-HT against Se-5HTR mediated phagocytosis. For dose-response analysis of
885 inhibitory compounds (0, 0.3, 3, 30, and 300 ng/larva), a fixed 5-HT concentration (1 μg/larva)
886 was used. For dose-response of 5-HT (0, 2, 20, 200 and 2,000 ng/larva), a fixed HB compound
887 concentration (1 μg/larva) was used. 'CON' represents a positive control without any inhibitor.
888
889 **Fig. 10. Specific inhibition of a designed compound (PhX) on Se-5HTR with a commercial**
890 **5-HTR$_7$ inhibitor (SB-269970) as reference in phagocytosis of *S. exigua*.** FITC-tagged *E. coli*
891 cells were injected to L5 larvae along with test chemicals. After 15 min, phagocytic cells were
892 observed under a fluorescent microscope at 400 × magnification and percentage of phagocytotic
893 hemocytes was calculated from randomly chosen 100 cells. Each treatment was independently
894 replicated three times. **(A)** Dose-response of PhX and SB-269970 with a fixed 5-HT
895 concentration (500 ng/larva). **(B)** Dose-response of 5-HT (0, 0.002, 0.02, 0.2, and 2 μg/larva)
896 with a fixed inhibitor concentration (10 ng/larva). 'CON' represents a positive control without
897 any inhibitor.

(A)

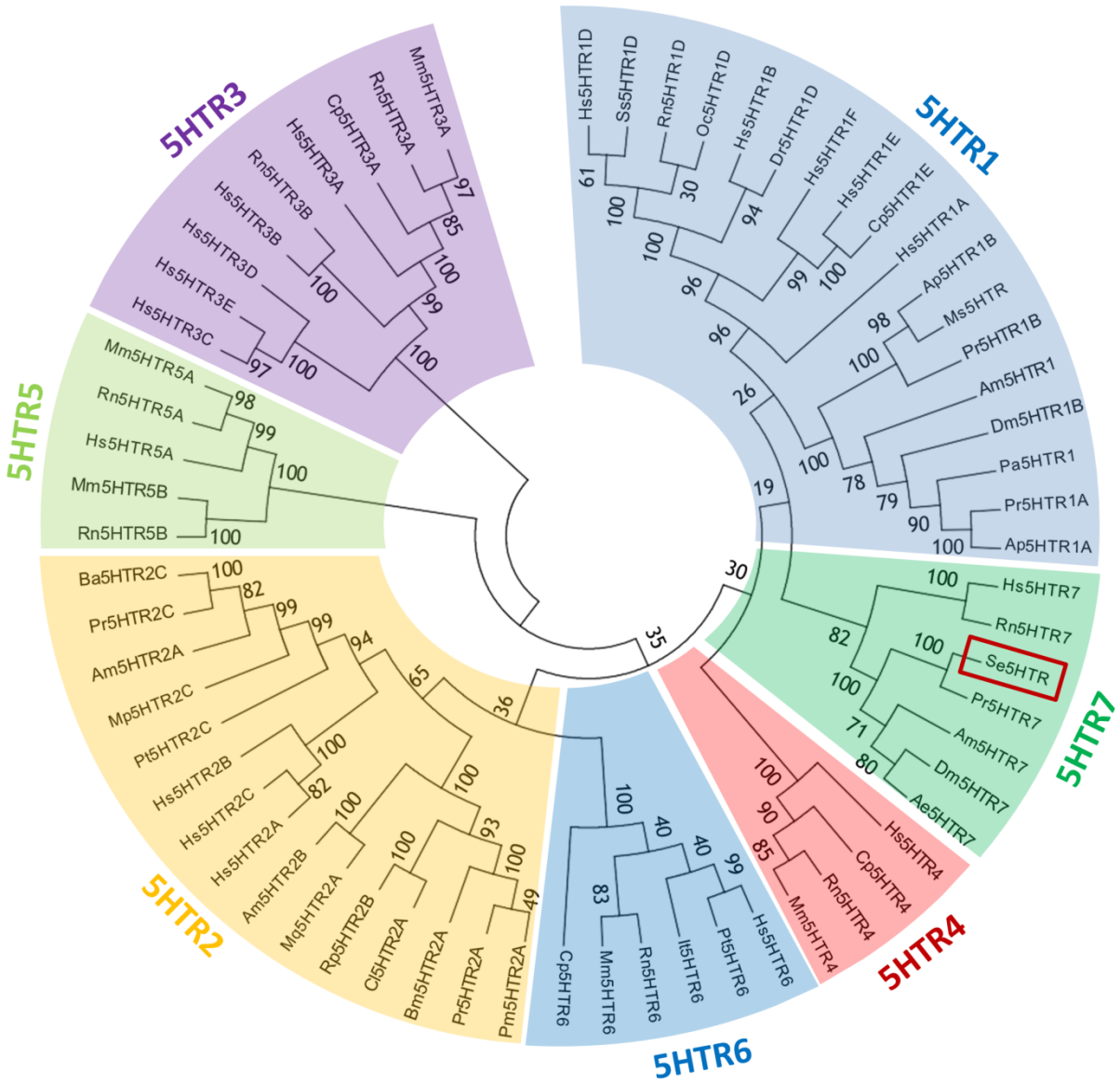
5HTR1
Hs5HTR1D
Ss5HTR1D
Rn5HTR1D
Oc5HTR1D
Hs5HTR1B
Dr5HTR1D
Hs5HTR1F
Hs5HTR1E
Cp5HTR1E
Hs5HTR1A
Ap5HTR1B
Ms5HTR
Pr5HTR1B
Am5HTR1
Dm5HTR1B
Pa5HTR1
Pr5HTR1A
Ap5HTR1A
5HTR3
Mm5HTR3A
Rn5HTR3A
Cp5HTR3A
Hs5HTR3A
Rn5HTR3B
Hs5HTR3B
Hs5HTR3D
Hs5HTR3E
Hs5HTR3C
5HTR5
Mm5HTR5A
Rn5HTR5A
Hs5HTR5A
Mm5HTR5B
Rn5HTR5B
5HTR7
Hs5HTR7
Rn5HTR7
Se5HTR
Pr5HTR7
Am5HTR7
Dm5HTR7
Ae5HTR7
5HTR4
Hs5HTR4
Cp5HTR4
Rn5HTR4
Mm5HTR4
5HTR6
Hs5HTR6
Pt5HTR6
Il5HTR6
Rn5HTR6
Mm5HTR6
Cp5HTR6
5HTR2
Ba5HTR2C
Pr5HTR2C
Am5HTR2A
Mp5HTR2C
Pt5HTR2C
Hs5HTR2B
Hs5HTR2C
Hs5HTR2A
Am5HTR2B
Mq5HTR2A
Rp5HTR2B
Cl5HTR2A
Bm5HTR2A
Pr5HTR2A
Pm5HTR2A

(B)

```
Se-5HTR   MAT--------QSHNSYCS---------LPSFVALPSCLLVLAS-ILLQF------------------------------ 32
Hs-5HTR7  -MMD--------VNSSGRP----------DLYGHIRSFLLPEVGRGLPDLS------------------------------ 32
Dm-5HTR7  MALSGQDWRRHQSHRQHRNHRTQGNHQKLISTATLTLFVLFLSSWIAYAAGKATVPAPLVEGETESATSQDFNSSSAFLG 80
Ms-5HTR7  MAT--------QNHKSHS----------LPSFVALPSCLLILVSILLLQFN------------------------------ 33
Pr-5HTR7  MAS--------QNNSHYS----------RPSLVTLSSYLLIFVSLVLQADS------------------------------ 33

                                                 *                 *
Se-5HTR   ALASVE----------------------LESILSPEFNVSNPNSTVNWTFLDDNSTFL--KHGHIKHSKYSI-------P 81
Hs-5HTR7  PDGGALP--------------------VAGSWAPHLLSEVTASPAPTWDAPFDNAS------GCGEQINYGR-------V 79
Dm-5HTR7  AIASASSTGSGSGSGSGSGSGSGSGSYGLASMNSSPIAIVSYQGITSSNLGDSNTTLVPLSDTPLLLEEFAAGEFVLPFL 160
Ms-5HTR7  AVDSVDC---------------------VDSLLASEYNYTNPNSTSNCTFFDTNST-----FKHIKHSKYST-------P 80
Pr-5HTR7  AFASFD----------------------FNSTFS-GVNTTNPNSTINWTFYDNNATVV--KHDHIKHLKYST-------L 81

                TM1                                TM2
                                   *                                          *
Se-5HTR   TTILLVTIFMIVIIGTIIGNVLVCVAVRLVRKLRRPSNYLIVSLAVSDLCVACIVMPVATVYDIMG-TWPFGPVICDFWV 160
Hs-5HTR7  EKVVIGSILTLITLLTIAGNCLVVISVCFVKKLRQPSNYLIVSLALADLSVAVAVMPFVSVTDLIGGKWIFGHFFCNVFI 159
Dm-5HTR7  TSIFVSIVLLIVILGTVVGNVLVCIAVCMVRKLRRPCNYLLVSLALSDLCVALLVMPMALLYEVLE-KWNFGPLLCDLWV 239
Ms-5HTR7  VTIFLVILFLIVIVCTIVGNILVCVAVRLVRKLRRPSNYLIVSLAVSDLCVAIIVMPFATVYDIMG-TWPFGPVICDFWA 159
Pr-5HTR7  VTVLLAAIFMVVIFGTIVGNILVCVAVCLVRKLRRPSNYLTVSLAVSDPCVAIMVMPVAMVYDLMG-SWPFGPVICDFWV 160

          TM3                                TM4
                                   *                                          *
Se-5HTR   SSDVLSCTASILNLCMISVDRYYAITKPLEYGVKRTPRRMLFCVFIVWISAAFISLPPVLILGNEKTDTS----CSVSQN 236
Hs-5HTR7  AMDVMCCTASIMTLCVISIDRYLGITRPLTYPVRQNGKCMAKMILSVWLLSASITLPPLFGWAQNVNDDK---VCLISCD 236
Dm-5HTR7  SFDVLCCTASILNLCAISVDRYLAITKPLEYGVKRTPRRMMLCVGIVWLAAACISLPPLLILGNEHEDEEGQPICTVCQN 319
Ms-5HTR7  SSDVLSCAASILNLCMISVDRYYAITKPLEYGVKRTPKRMLLCILIVWMSAAFISLPPVLILGNEKTPTS----CSVSQN 235
Pr-5HTR7  SSDVLSCAASILNLCMISVDRYYAITKPLEYGVKRTPRRMLFCVFIVWMSAAFISLPPVLILGNEKSDTS----CSVSQN 236

          TM5
                *
Se-5HTR   QAYQIYATFGSFYIPLTVMIVVYYKIFRAARKIVKDEKR-AQSHLETHCYLEIN-------VKNGGAAEAKLLGNQP-AQ 307
Hs-5HTR7  FGYTIYSTAVAFYIPMSVMLFMYYQIYKAARKSAAKHKFPGFPRVEPDSVIALNGIVKLQKEVEECANLSRLLKHERKNI 316
Dm-5HTR7  FAYQIYATLGSFYIPLSVMLFVYYQIFRAARRIVLEEKR-AQTHLQ---QALNG-------TGSPSAPQAPPLGHT---E 385
Ms-5HTR7  QVYQIYATLGSFYIPLTVMVVVYYKIFRAARKIVKDEKR-AQSHLETHCYLEIN-------VKNGGAAEAKLLGNQPAAQ 307
Pr-5HTR7  QGYQIYATFGSFYLPLTVMVVVYYKIFSAARKIVKDERR-AQSHLESHCYLEIN-------VKNGGAAEAKLLGNQP--Q 306

                *         *                                *       ▲
Se-5HTR   PPPRGSTASTNTTCSVDKTESTIGRCFSGQRKSNESQC--PMLQQPKTPTKPIHTINRSPTQLVPGKLAVKERQRQPSES 385
Hs-5HTR7  SIFKREQKAATTLGIIVGAFTVCWLPFFLLSTARPFICGTSCSCIFLWVERTFLWLGYANSLINPFIYAFFNRDLRTTYR 396
Dm-5HTR7  LASSGNGQRHSSVGNTSLTYSTCGGLSSG---------------------------------------------------- 414
Ms-5HTR7  PPPRGSTASTNTTCSVDKAESGLGRCFSGQRKSNESQC--PMLQQPKTPTKPIHTINRSPTTLTPNNKPIVKDRRRPSET 385
Pr-5HTR7  NPTRGSTASTNTTCSVDKAENSIGRCFSG-RKSNESQC--PMLQPPKTLTKPIHTINR-PASQNLNPDSNLKERRRPSSD 382

                                                                                TM6
                          *  *                                  *
Se-5HTR   SQKNTTNR---IRSSLSNFAHKSHIAKDLLHPQNAVHQKKLRFQLAKERKASTTLGIIMSAFVICWLPFFVLALIRPFVK 462
Hs-5HTR7  SLLQCQYRNINRKLSAAGMHEALKLAERPERPEFVLRACTRRVLLRPEKRPPVSVWVLQSPDHHNWLADKMLTTVEKKVM 476
Dm-5HTR7  -----------GGALAGHGSGGGVSGSTGLLG-SPHHKKLRFQLAKEKKASTTLGIIMSAFTVCWLPFFILALIRPFET 481
Ms-5HTR7  SNKMTTNR---IRSSLSNFAQKSHIAKDLFHSQ-SSHQKKLRFQLAKERKASTTLGIIMSAFIICWLPFFVLALIRPFVE 461
Pr-5HTR7  NQKQTS-R---IRSSLSTFAHKSHIAKDLLHPVNSPHQKKLRFHLAKERKASTTLGIIMSAFIVCWLPFFVLALIRPFVN 458

                TM7
                                                                                ▼       ▼▲*
Se-5HTR   EDAIPDAVSALFLWLGYLNSLLNFVIYATLNRDFRKPFQEILFFRCGNLNHMMREEFYHSQYGDPDQHYCVNNTTKMHNY 542
Hs-5HTR7  IHD                                                                          ------- 549
Dm-5HTR7  MH-VPASLSSLFLWLGYANSLLNPIIYATLNRDFRKPFQEILYFRCSSLNTMMRENYYQDQYGEPPSQRVMLG------- 553
Ms-5HTR7  EDAIPDAVSALFLWLGYLNSLLNPIIYATLNRDFRKPFQEILFFRCSNLNHMMREEFYHSQYGDPDQHYCGNNTTKLHNY 541
Pr-5HTR7  EDTIPDAVSALFLWLGYLNSLLNPIIYATLNRDFRKPFQEILFFRCSNLNHMMREEFYHSQYGGPEPHYCVNNS-KNQNY 537

                          *
Se-5HTR   EEGVEIVSAVDREETRASESFL                                                          564
Hs-5HTR7  -------                                                                         564
Dm-5HTR7  -------D--ER--HGARESFL                                                          564
Ms-5HTR7  DEGVEIVSAIDREETRASESFL                                                          564
Pr-5HTR7  DEGVEIVSAVDREETRATESFL                                                          564
```

Fig. 1

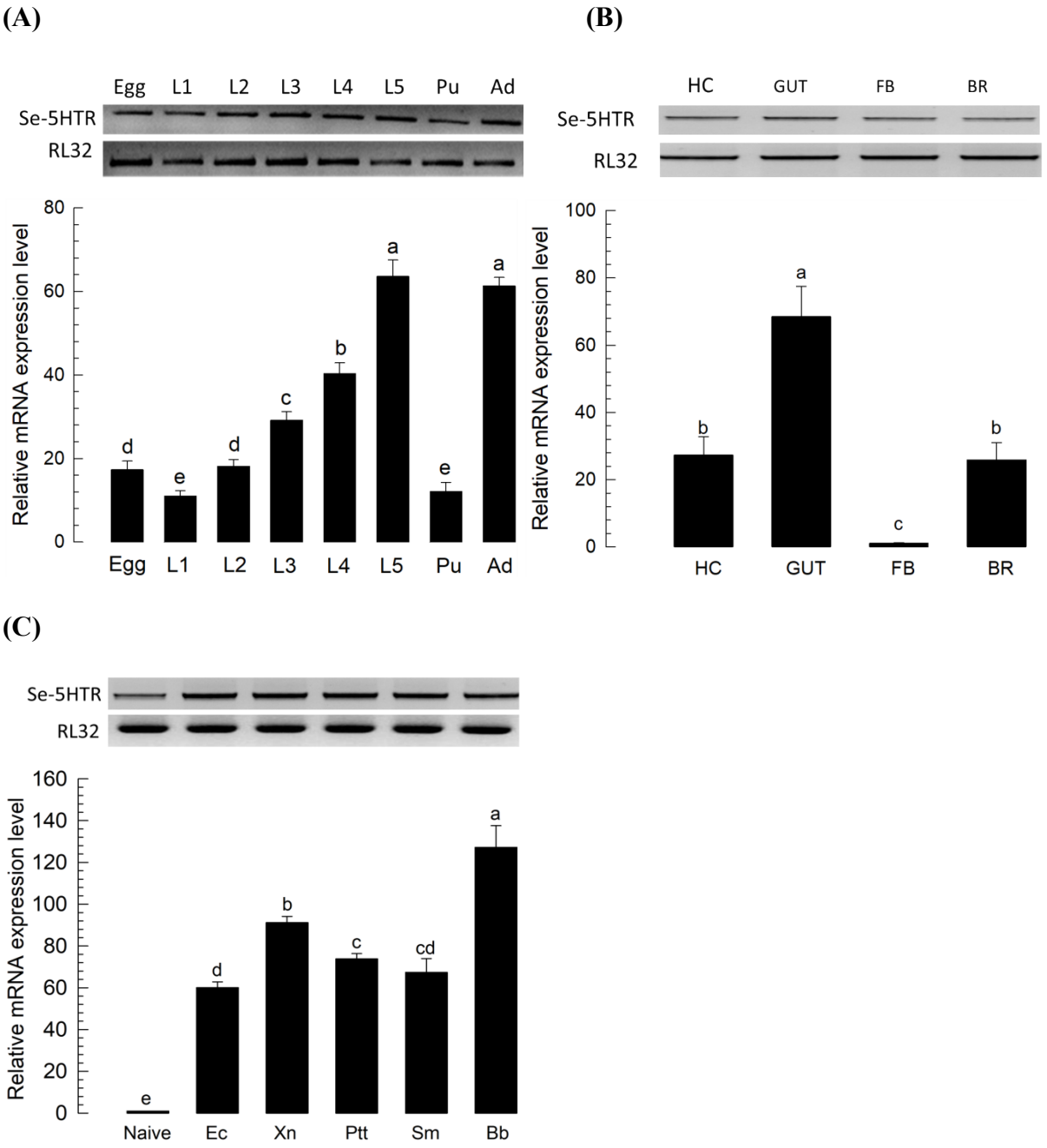
(A)
Egg L1 L2 L3 L4 L5 Pu Ad
Se-5HTR
RL32
Relative mRNA expression level
0 20 40 60 80
d e d c b a e a
Egg L1 L2 L3 L4 L5 Pu Ad
(B)
HC GUT FB BR
Se-5HTR
RL32
Relative mRNA expression level
0 20 40 60 80 100
b a c b
HC GUT FB BR
(C)
Se-5HTR
RL32
Relative mRNA expression level
0 20 40 60 80 100 120 140 160
e d b c cd a
Naive Ec Xn Ptt Sm Bb

Fig. 2

(A)

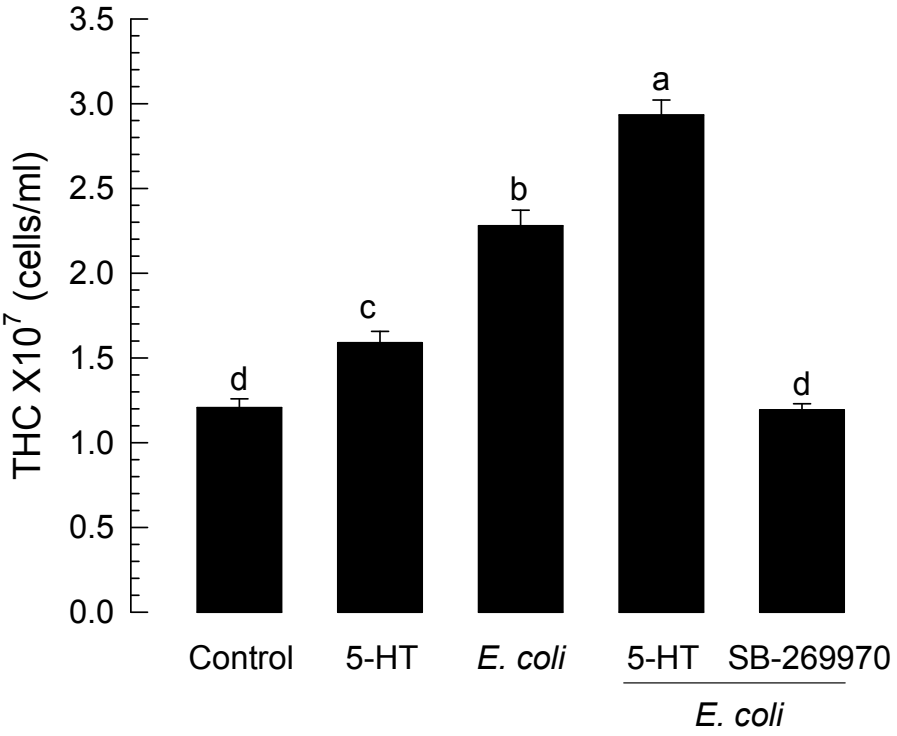
3.5
3.0
2.5
2.0
1.5
1.0
0.5
0.0
THC X10^7 (cells/ml)
a
b
c
d
d
Control
5-HT
E. coli
5-HT
SB-269970
E. coli

(B)

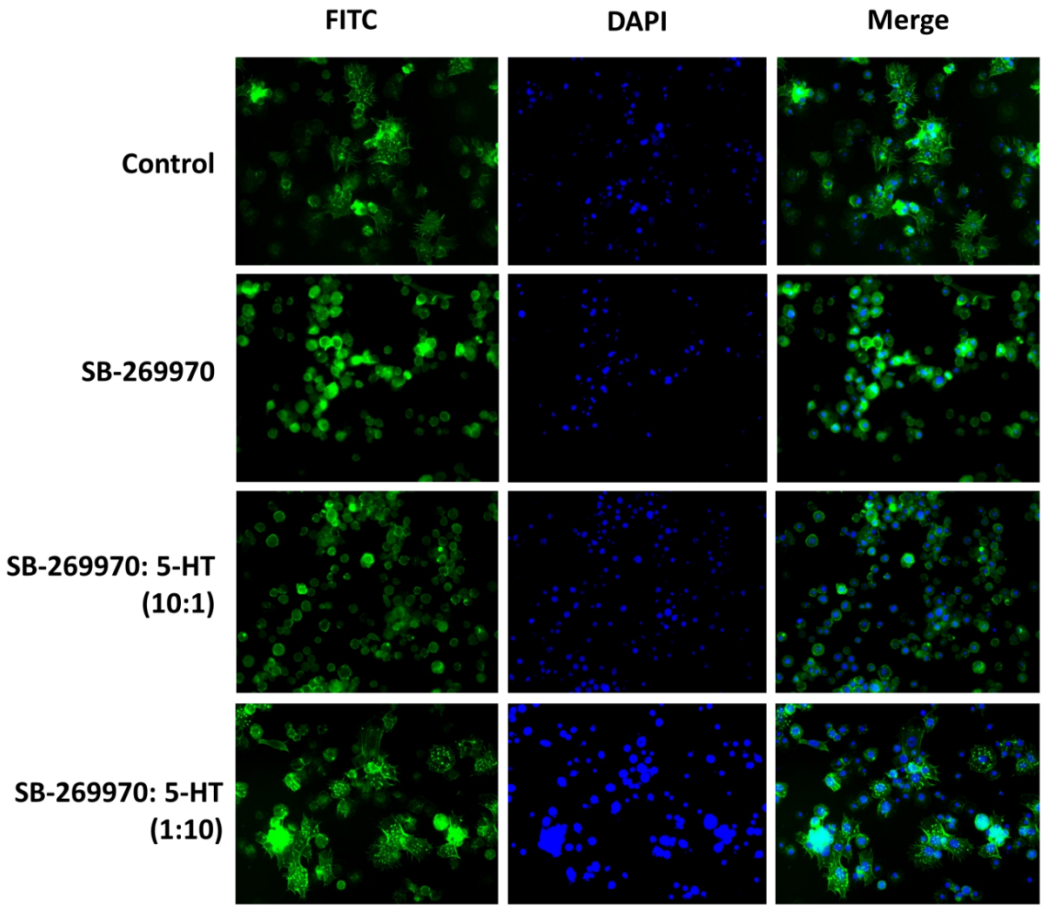
FITC
DAPI
Merge
Control
SB-269970
SB-269970: 5-HT (10:1)
SB-269970: 5-HT (1:10)

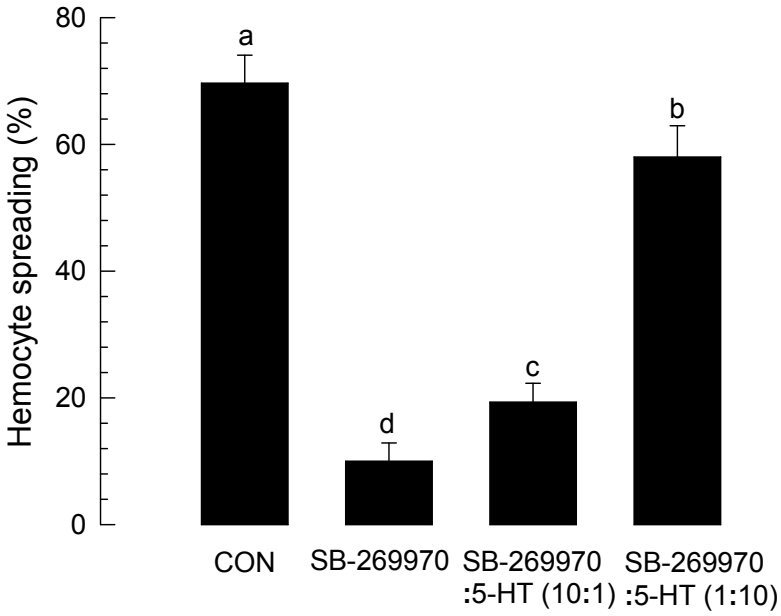
Hemocyte spreading (%)
80
60
40
20
0
a
d
c
b
CON
SB-269970
SB-269970 :5-HT (10:1)
SB-269970 :5-HT (1:10)

Fig. 3

(A)

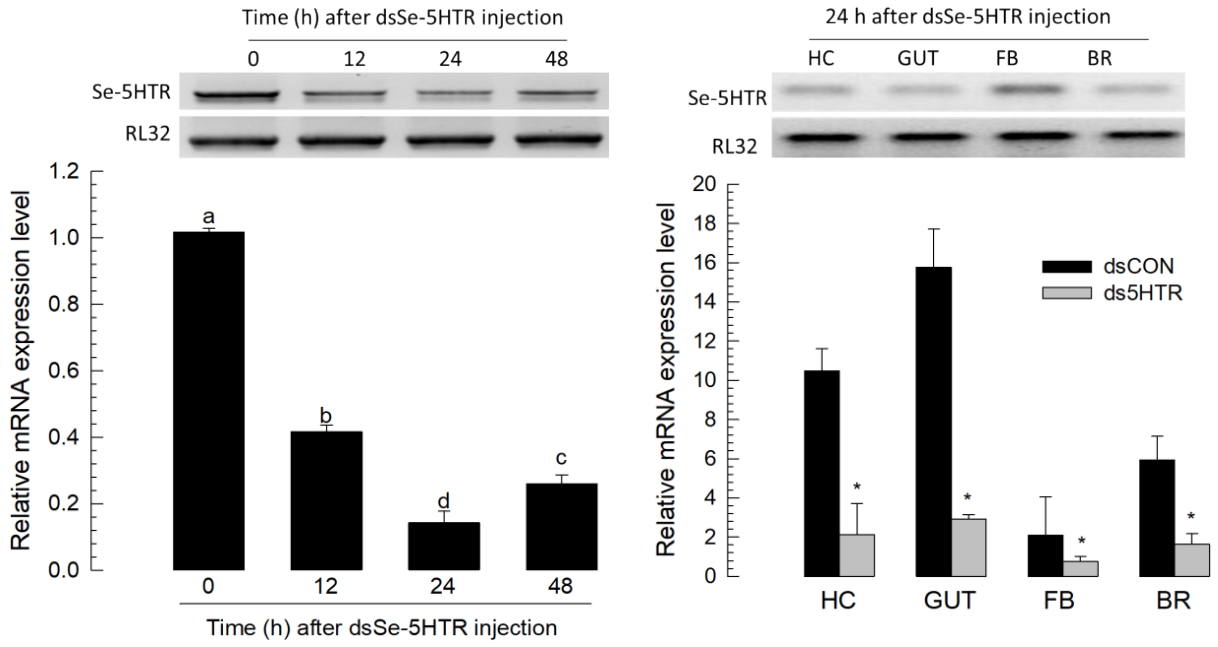
Time (h) after dsSe-5HTR injection
0
12
24
48
Se-5HTR
RL32
Relative mRNA expression level
1.2
1.0
0.8
0.6
0.4
0.2
0.0
a
b
d
c
0
12
24
48
Time (h) after dsSe-5HTR injection
24 h after dsSe-5HTR injection
HC
GUT
FB
BR
Se-5HTR
RL32
Relative mRNA expression level
20
18
16
14
12
10
8
6
4
2
0
dsCON
ds5HTR
*
HC
GUT
FB
BR

(B)

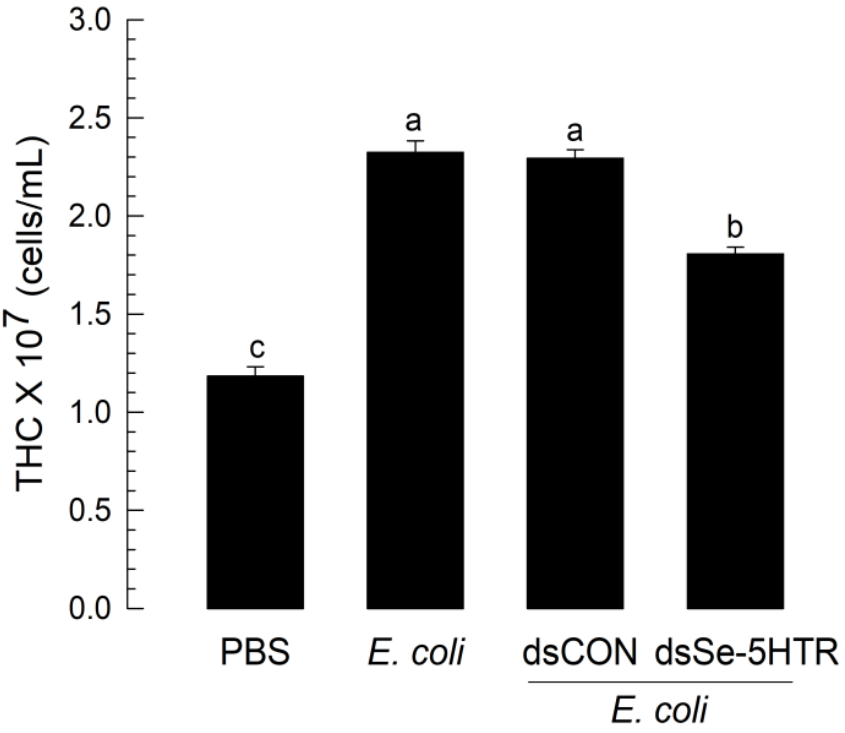
THC X 10^7 (cells/mL)
3.0
2.5
2.0
1.5
1.0
0.5
0.0
c
a
a
b
PBS
E. coli
dsCON
dsSe-5HTR
E. coli

(C)

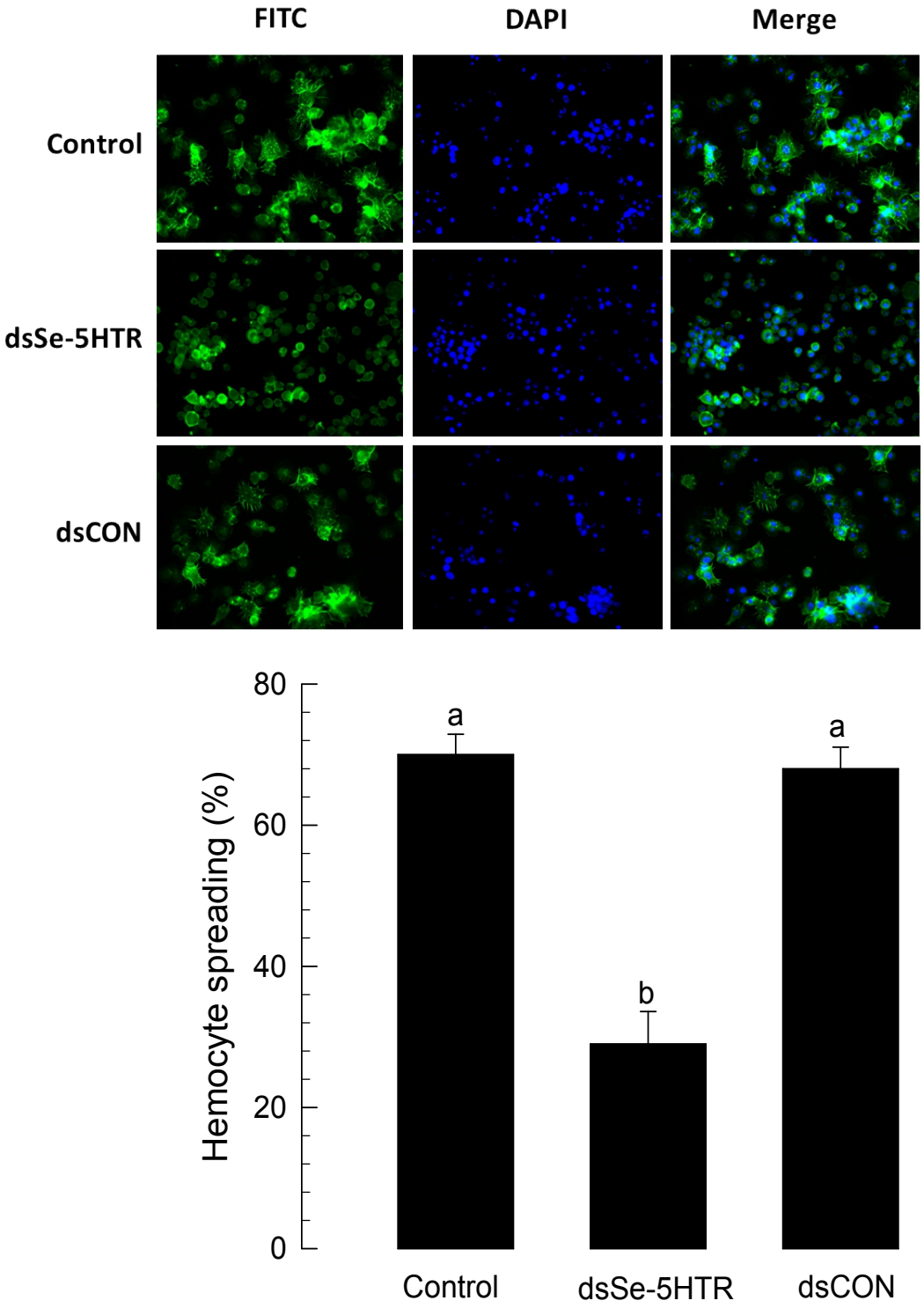
FITC
DAPI
Merge
Control
dsSe-5HTR
dsCON
Hemocyte spreading (%)
80
60
40
20
0
a
b
a
Control
dsSe-5HTR
dsCON

Fig. 4

(A)

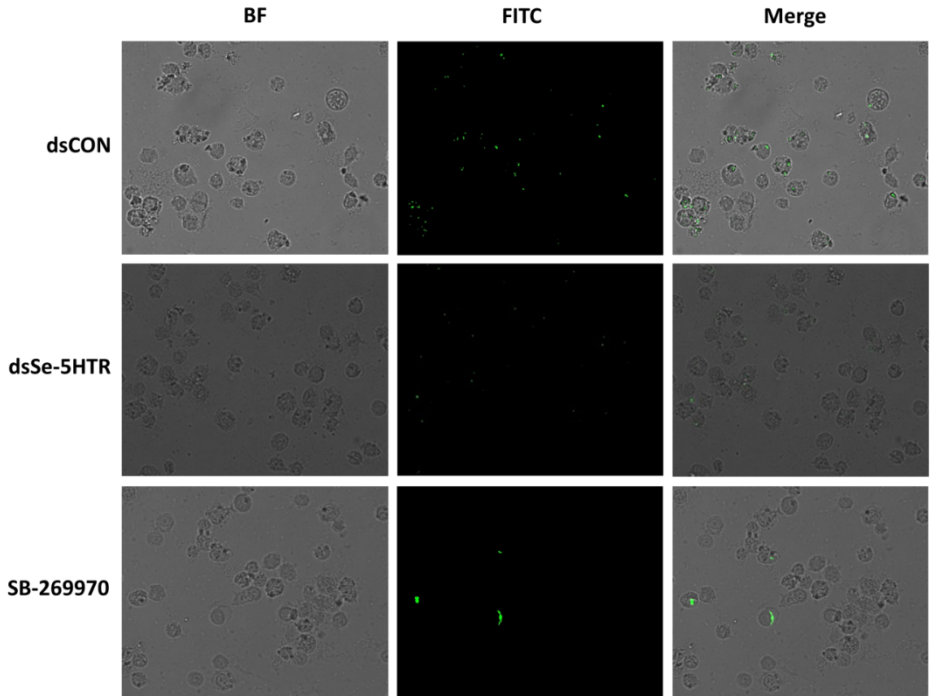
BF
FITC
Merge
dsCON
dsSe-5HTR
SB-269970

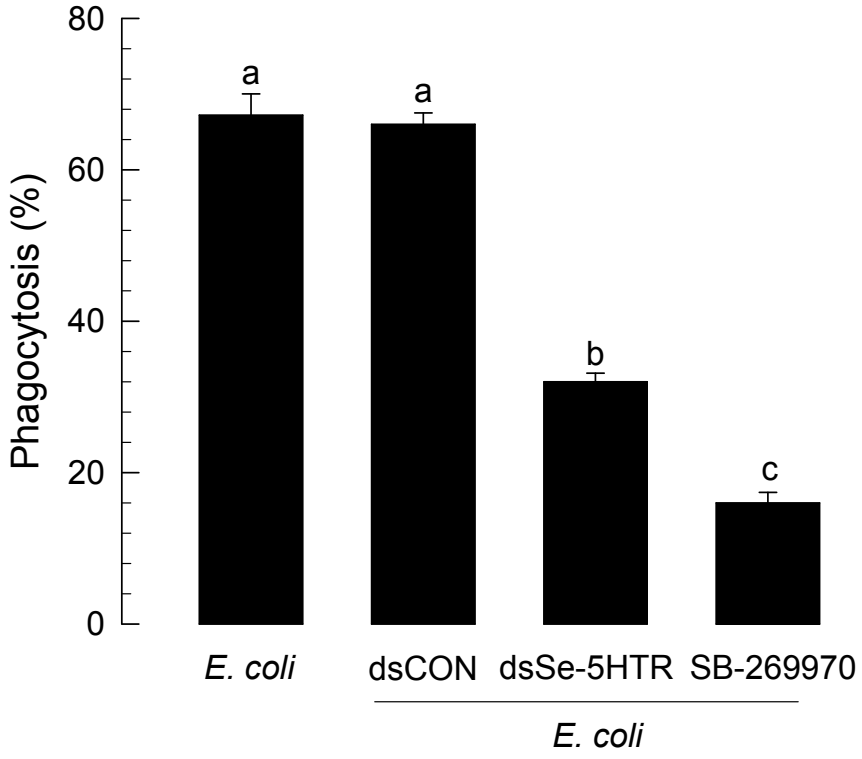
Phagocytosis (%)
80
60
40
20
0
a
a
b
c
E. coli
dsCON
dsSe-5HTR
SB-269970
E. coli

(B)

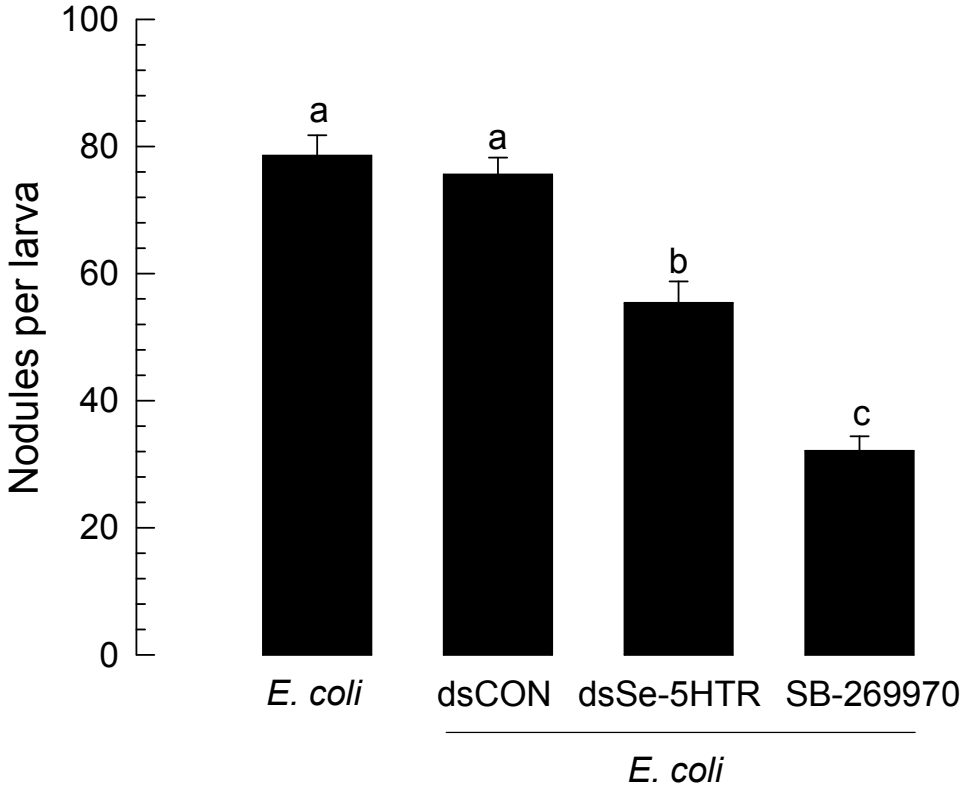
100
80
60
40
20
0
Nodules per larva
a
a
b
c
E. coli
dsCON
dsSe-5HTR
SB-269970
E. coli

Fig. 5

(A)

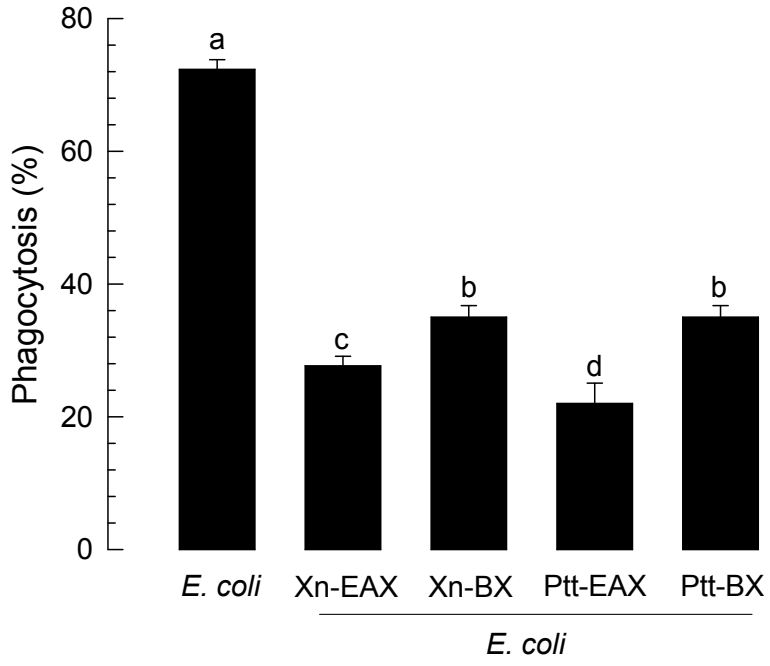
Phagocytosis (%)
80
60
40
20
0
a
c
b
d
b
E. coli
Xn-EAX
Xn-BX
Ptt-EAX
Ptt-BX
E. coli

(B)

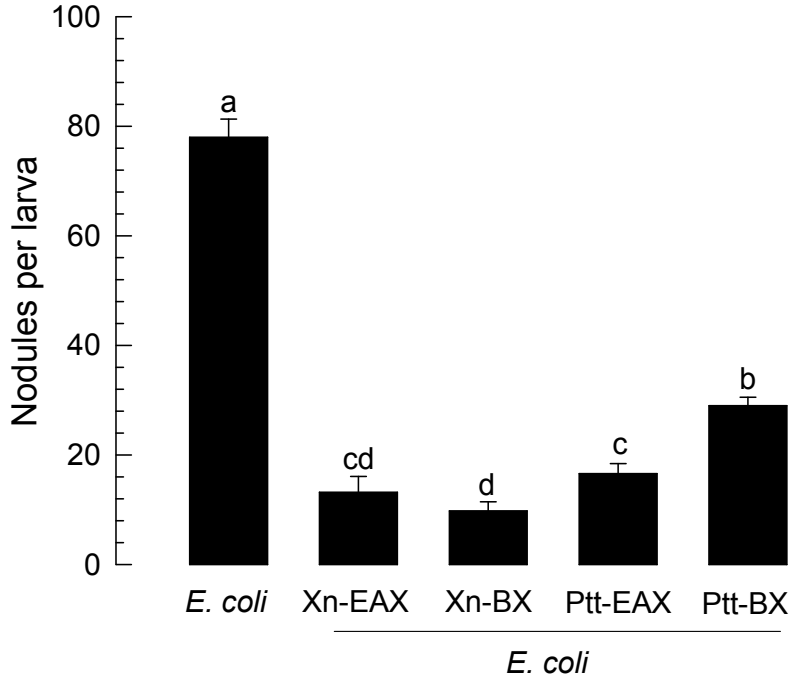
Nodules per larva
100
80
60
40
20
0
a
cd
d
c
b
E. coli
Xn-EAX
Xn-BX
Ptt-EAX
Ptt-BX
E. coli

Fig. 6

(A)

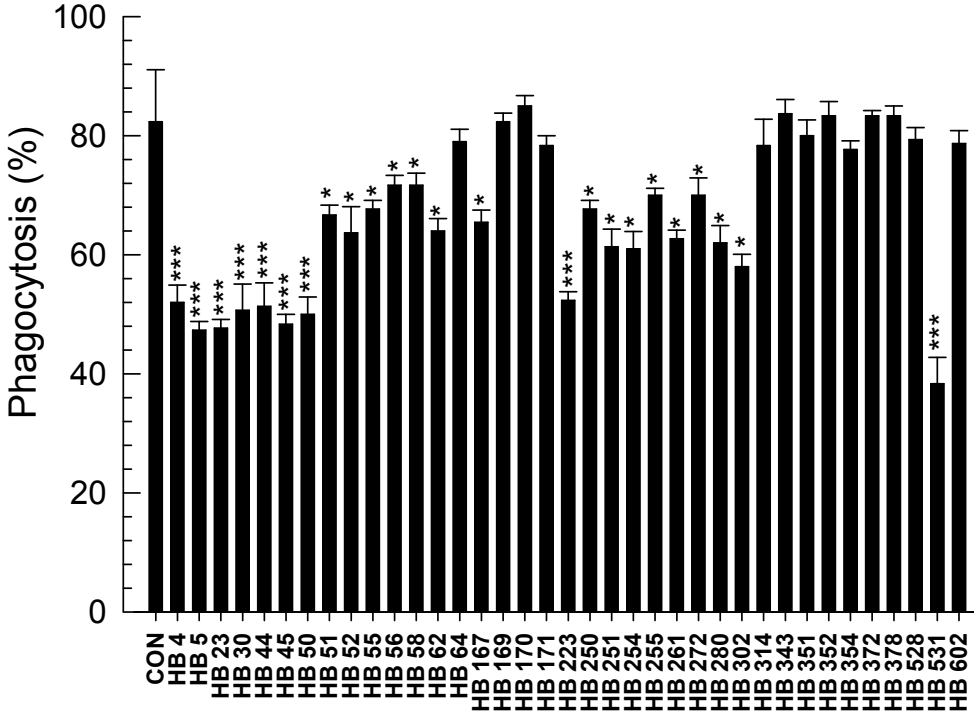
Phagocytosis (%)
100
80
60
40
20
0
CON
HB 4
HB 5
HB 23
HB 30
HB 44
HB 45
HB 50
HB 51
HB 52
HB 55
HB 56
HB 58
HB 62
HB 64
HB 167
HB 169
HB 170
HB 171
HB 223
HB 250
HB 251
HB 254
HB 255
HB 261
HB 272
HB 280
HB 302
HB 314
HB 343
HB 351
HB 352
HB 354
HB 372
HB 378
HB 528
HB 531
HB 602

(B)

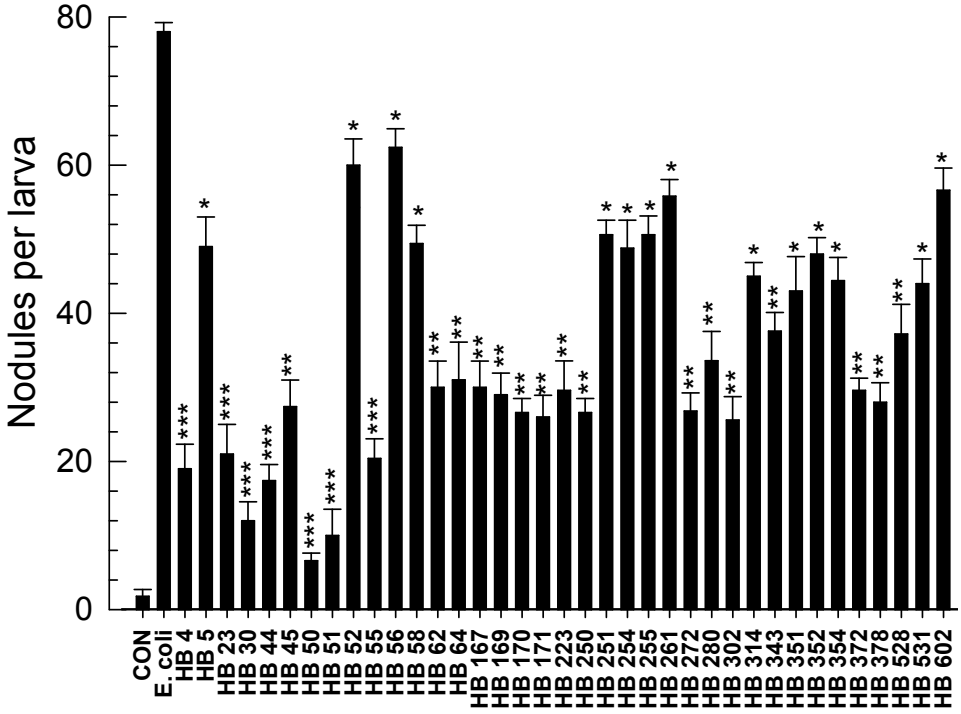
Nodules per larva
80
60
40
20
0
CON
E. coli
HB 4
HB 5
HB 23
HB 30
HB 44
HB 45
HB 50
HB 51
HB 52
HB 55
HB 56
HB 58
HB 62
HB 64
HB 167
HB 169
HB 170
HB 171
HB 223
HB 250
HB 251
HB 254
HB 255
HB 261
HB 272
HB 280
HB 302
HB 314
HB 343
HB 351
HB 352
HB 354
HB 372
HB 378
HB 528
HB 531
HB 602

Fig. 7

(A)

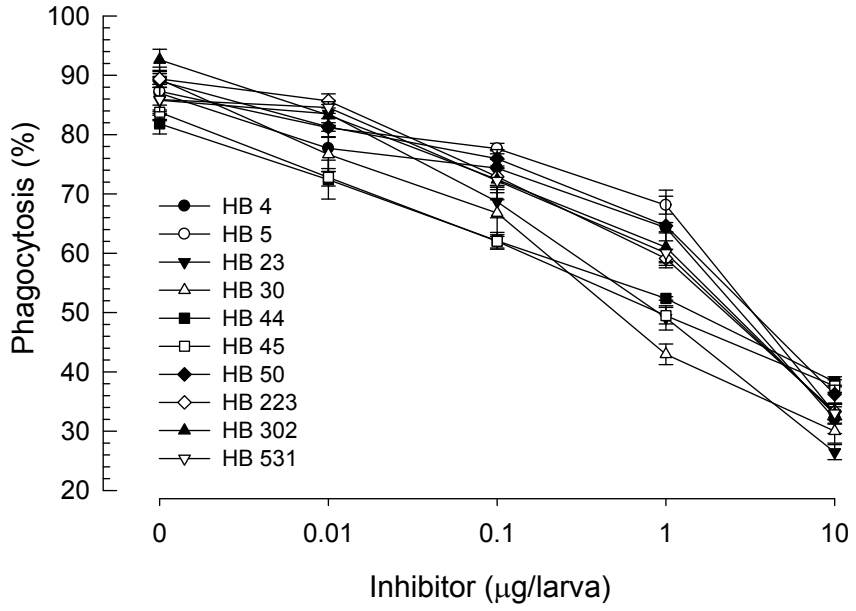
Phagocytosis (%)
100
90
80
70
60
50
40
30
20
HB 4
HB 5
HB 23
HB 30
HB 44
HB 45
HB 50
HB 223
HB 302
HB 531
0
0.01
0.1
1
10
Inhibitor (μg/larva)

(B)

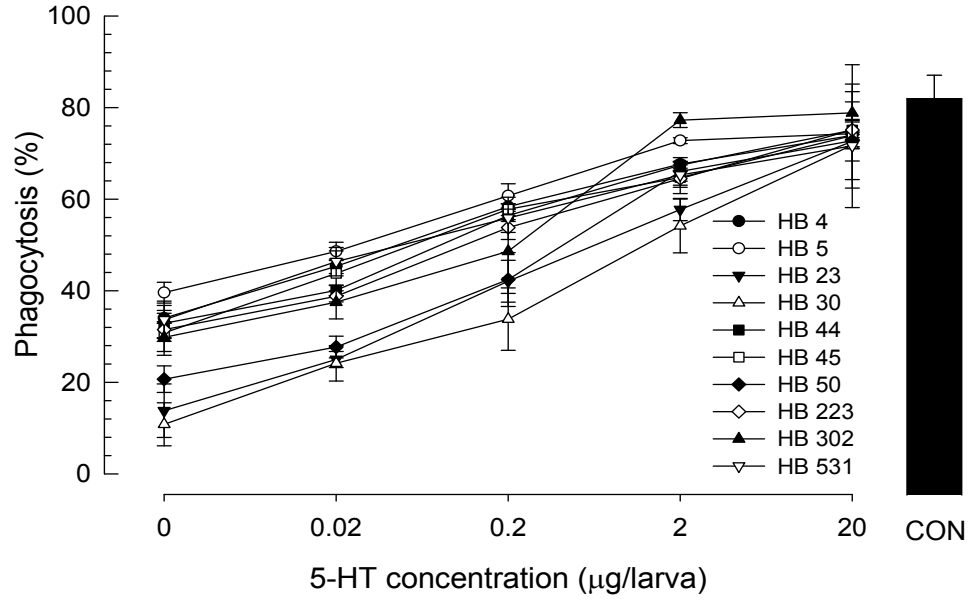
Phagocytosis (%)
100
80
60
40
20
0
HB 4
HB 5
HB 23
HB 30
HB 44
HB 45
HB 50
HB 223
HB 302
HB 531
0
0.02
0.2
2
20
CON
5-HT concentration (μg/larva)

Fig. 8

(A)

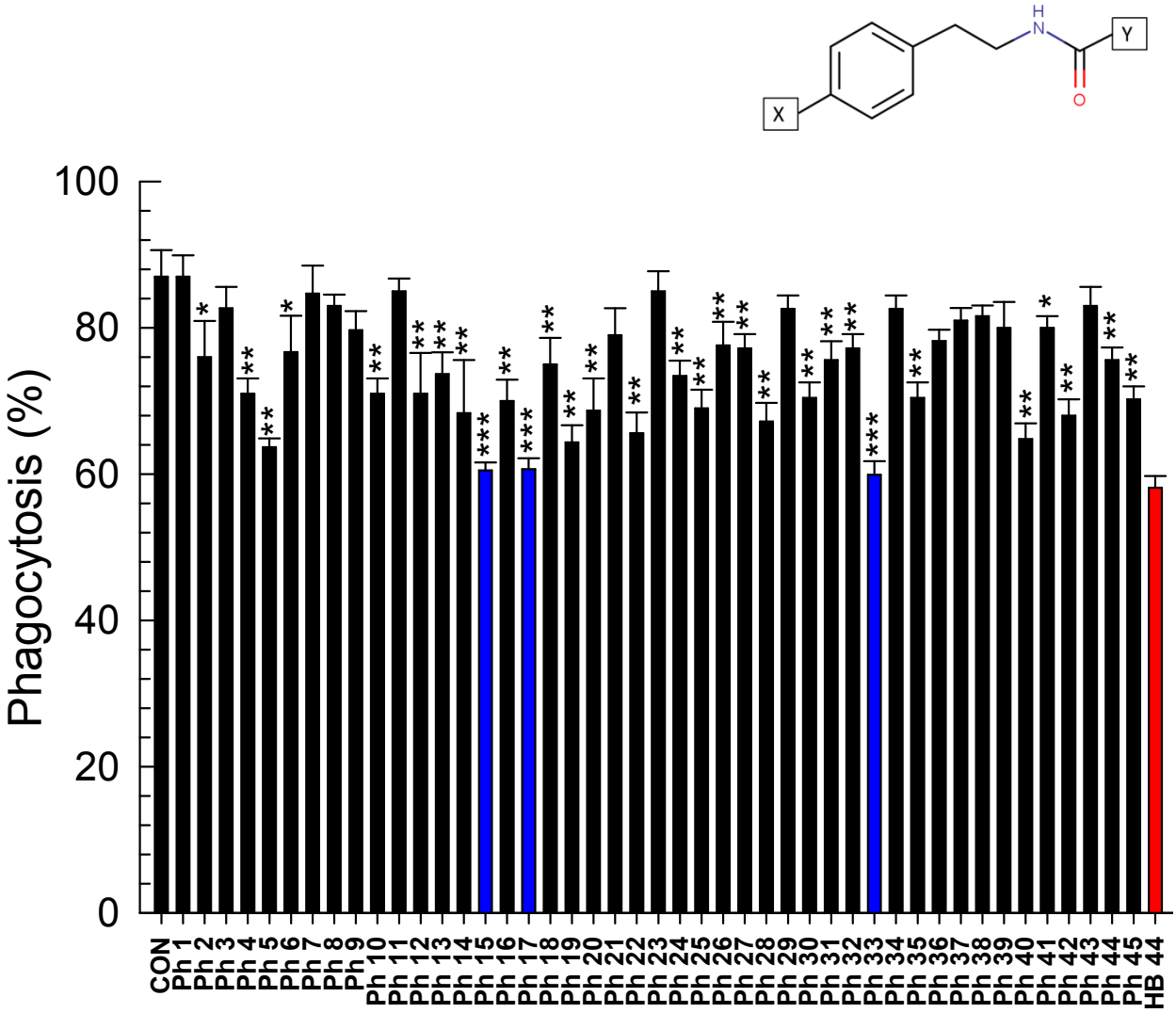

(B)

Compound	Structure	IC_{50} (μM)
Ph 15	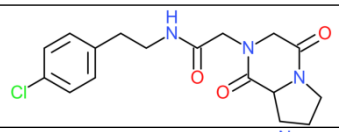	1.862 ± 0.221[c]
Ph 17	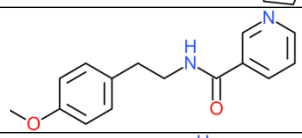	2.746 ± 0.078[b]
Ph 33	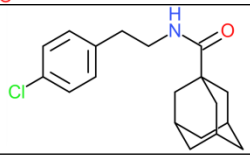	5.587 ± 0.98[a]

(C)

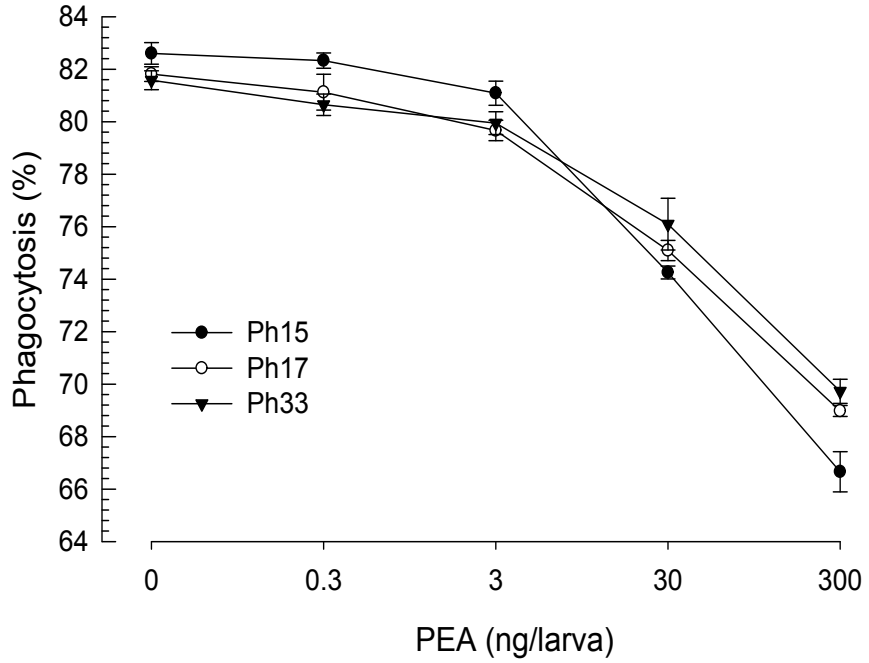
84
82
80
78
76
74
72
70
68
66
64
Phagocytosis (%)
Ph15
Ph17
Ph33
0
0.3
3
30
300
PEA (ng/larva)

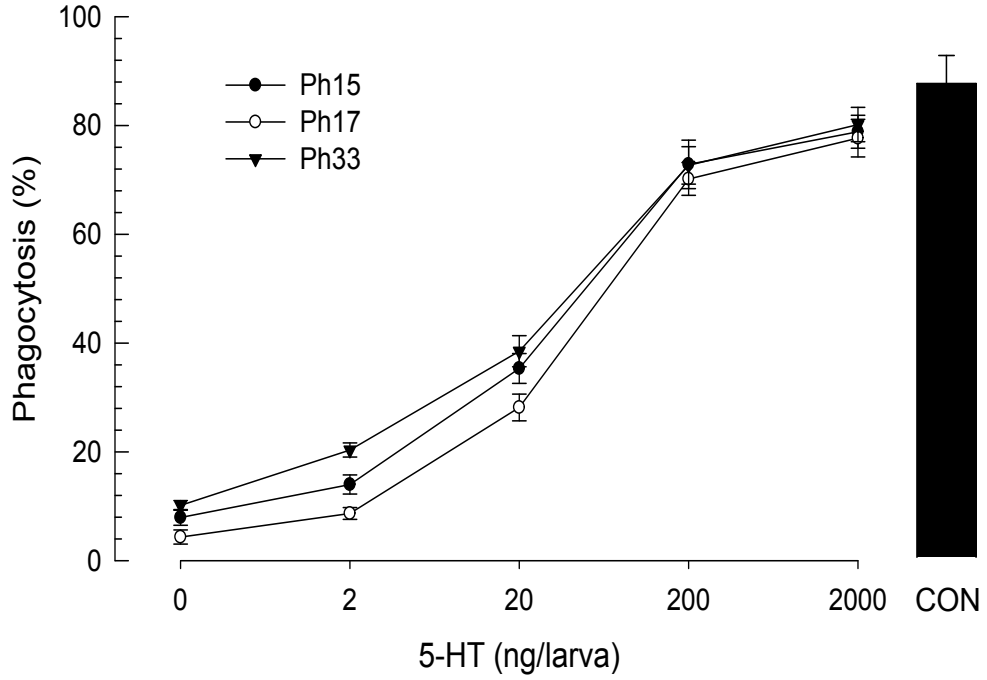
100
80
60
40
20
0
Phagocytosis (%)
Ph15
Ph17
Ph33
0
2
20
200
2000
CON
5-HT (ng/larva)

Fig. 9

(A)

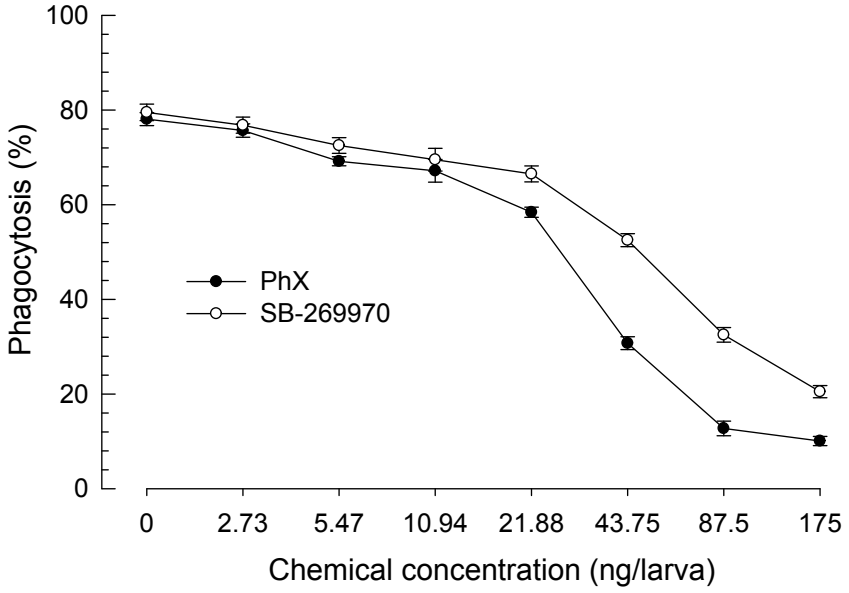
100
80
60
40
20
0
Phagocytosis (%)
PhX
SB-269970
0
2.73
5.47
10.94
21.88
43.75
87.5
175
Chemical concentration (ng/larva)

(B)

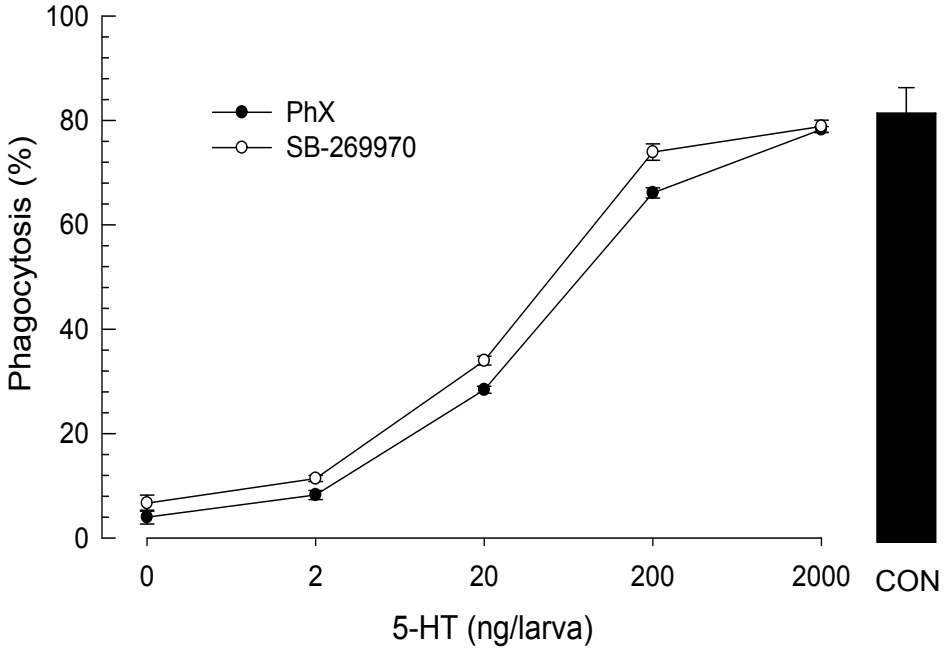
100
80
60
40
20
0
Phagocytosis (%)
PhX
SB-269970
0
2
20
200
2000
CON
5-HT (ng/larva)

Fig. 10

Supplementary data

S1 Fig. Putative domain and motif structures of Se-5HTR. Putative seven transmembrane domains (TM1-TM7) are primarily marked by dark yellow bars and circles. Extracellular and cytosolic regions are denoted by green and light blue regions, respectively. Potential N-glycosylation sites and phosphorylation sites are marked by orange and red circles, respectively. Aspartic acid residue (dark blue circle) in TM3 and serine residue (light brown circle) in TM5 are putative residues that might chemically interact with 5-HT. The unique consensus sequence motif (PXXXWXPXF, dark brown circles) in aminergic receptors is conserved in TM6. The motif (NPXXY, dark blue circles) is conserved in TM7 like other GPCRs. Two possible post-translational palmitoylation cysteine residues (light yellow circles) and a PDZ-domain binding motif (ESFL, black circles) are also present in the C-terminal. Conserved motifs were determined using InterPro tool (https://www.ebi.ac.uk/interpro/) and Prosite (http://prosite.expasy.org/) whereas other residues and motifs were predicted using several tools from DTU bioinformatics.

S2 Fig. Potent screened chemicals from HB compounds with their chemical structures and respective median inhibitory concentrations (IC_{50}). HB chemicals were injected in different doses (0, 0.01, 0.1, 1, and 10 µg/larva) along with a fixed 5-HT concentration (1 µg/larva) and FITC-tagged bacteria (500 cells/larva). After 15 min of treatment, hemocytes from treated larvae were collected in ACB followed by phagocytosis assay as described above. Percentages of phagocytosis against HB chemical treatment with increasing concentrations were calculated. Their IC_{50} values were determined using Probit analysis (https://probitanalysis.wordpress.com).

S3 Fig. Designing a potent chemical inhibitor from phenylehtylamide (PEA) derivatives. Derivatives of PEA were tested for their nodulation inhibition percentages and sorted by their X and Y groups. Most potent residues inhibiting nodulation were selected and a hypothetical most potent PEA chemical was designed. (A) Core PEA structure with two variable hypothetical residues (X and Y). X belongs to the residue group attached with para position of the phenyl ring whereas Y belongs to the residue group linked to the amide group. (B) Comparative analysis between X residue groups with their mean percent inhibition of nodulation. (C) Comparative analysis between Y residue groups with their percent inhibition of nodulation. (D) A hypothetical PEA chemical compound structure having the most potent inhibition capability.

S4 Fig. Bacterial secondary metabolites (37 chemicals) derived from *Xenorhabdus* and *Photorhabdus*

S5 Fig. Phenylethylamide (PEA) derivatives (45 chemicals) based on HB 44, a bacterial metabolite

S6 Fig. Chemical synthesis of PhX ((*S*)-2-(1,4-dioxohexahydropyrrolo[1,2-*a*]pyrazin-2(*1H*)-yl)-*N*-(4-methoxyphenethyl)acetamide)

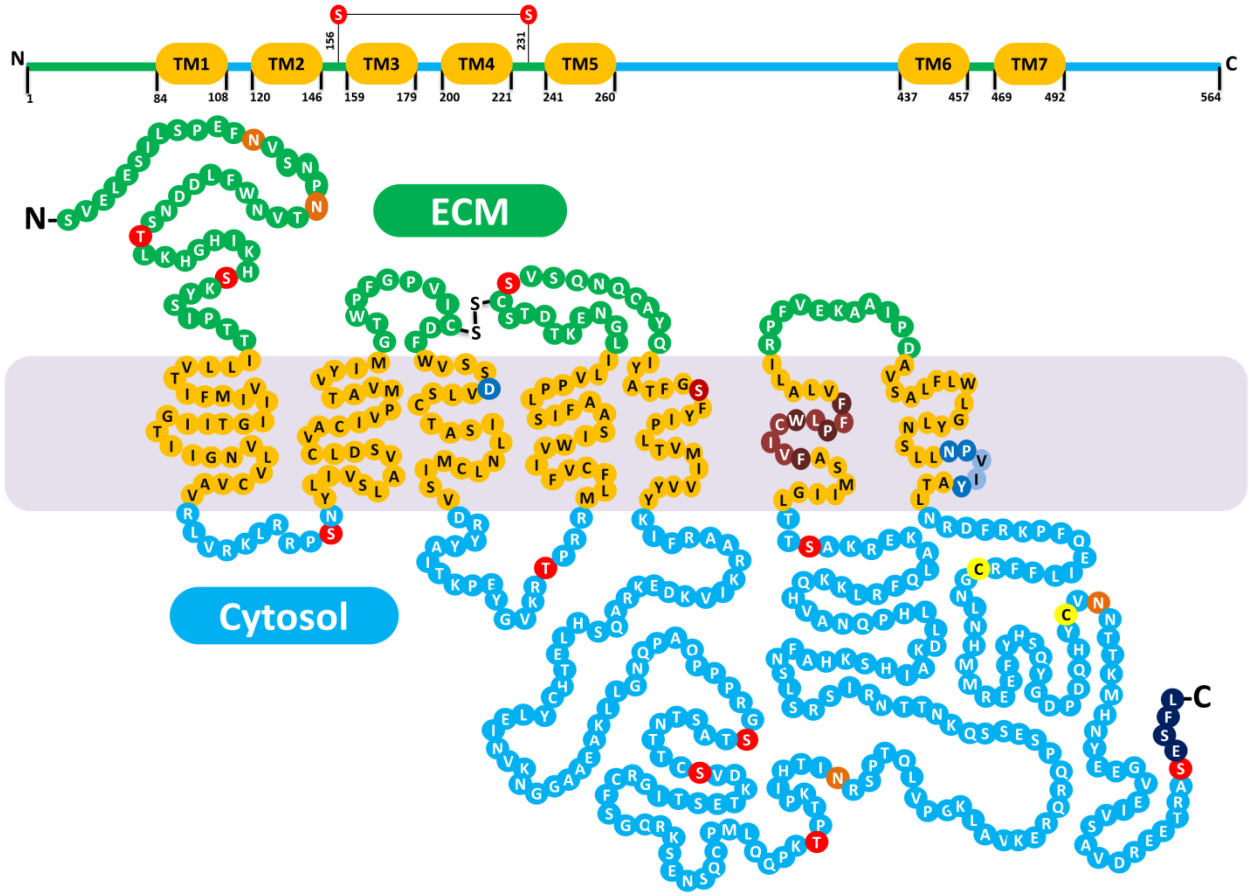
N
C
TM1
TM2
TM3
TM4
TM5
TM6
TM7
1
84
108
120
146
156
159
179
200
221
231
241
260
437
457
469
492
564
ECM
Cytosol

S1 Fig

Groups	ID	Structure	IC_{50} (μM)
Phenylethylamide	HB 4		253.2 ± 38.0
	HB 5		217.8 ± 43.6
	HB 44		103.7 ± 18.7
Tryptamide	HB 23		103.9 ± 15.6
	HB 50		90.6 ± 16.3
	HB 531		124.9 ± 23.7
Xenortide	HB 30		59.1 ± 9.5
Xenocyloin	HB 45		82.1 ± 14.8
Nematophin	HB 223		134. 6 ± 22.9
GameXPeptide	HB 302		58.4 ± 11.7

S2 Fig

(A)

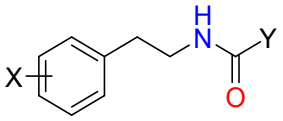

(B)

X	N	Inhibition of nodulation
4-OCH_3	2	80.9%
3,4-di-OCH_3	1	53.4%
4-Cl	3	49.6%
4-F	1	72.1%
4-CF_3	1	66.9%
4-H	2	62.7%

(C)

Y	Inhibition of nodulation
(X=4-Cl)	
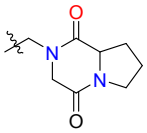	84.1%
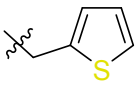	36.3%
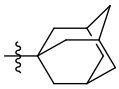	35.1%
(X=3,4-di-OMe)	
	77.7%
	77.3%
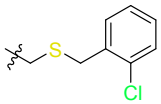	53.4%
(X=4-F)	
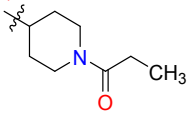	72.1%
(X=4-CF_3)	
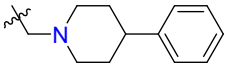	66.9%
(X=4-H)	
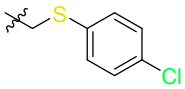	64.1%
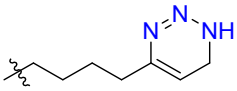	61.4%

(D)

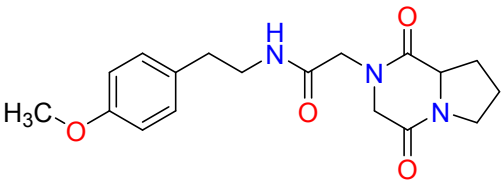

S3 Fig

HB compound	Structure
HB 4	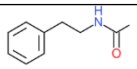
HB 5	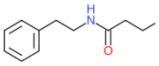
HB 23	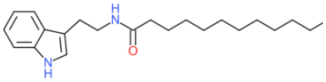
HB 30	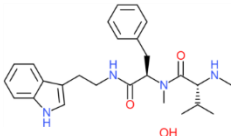
HB 44	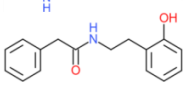
HB 45	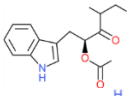
HB 50	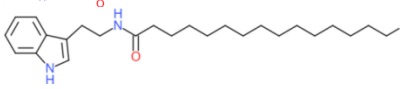
HB 51	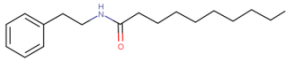
HB 52	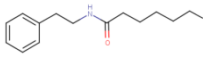
HB 55	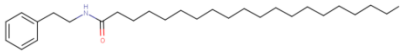
HB 56	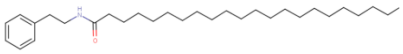
HB 58	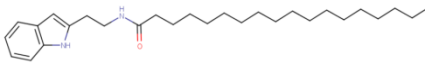

HB compound	Structure
HB 250	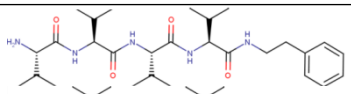
HB 251	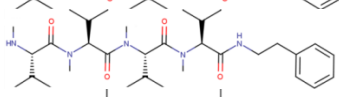
HB 254	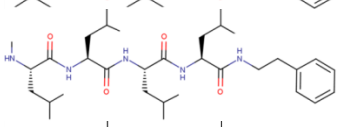
HB 255	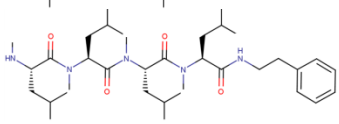
HB 261	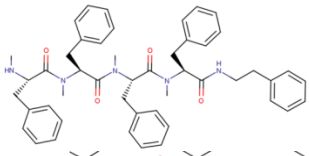
HB 272	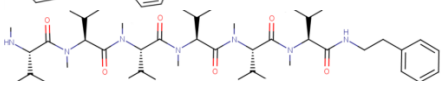
HB 280	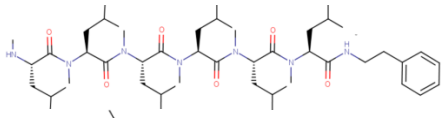
HB 302	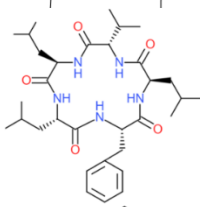
HB 314	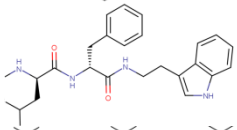
HB 343	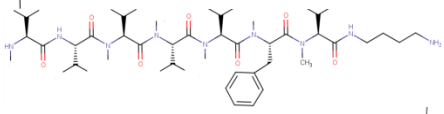
HB 351	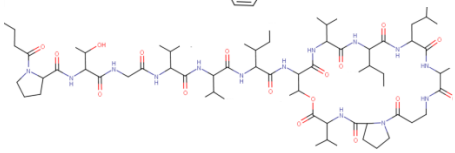
HB 352	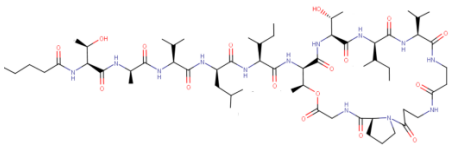

HB 62

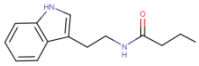

HB 64

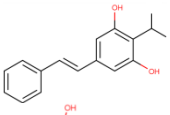

HB 167

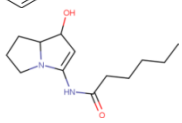

HB 169

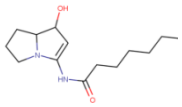

HB 170

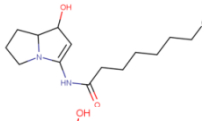

HB 171

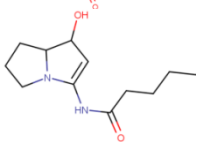

HB 223

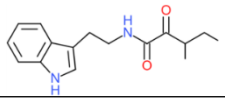

HB 354

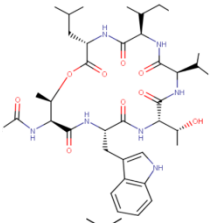

HB 372

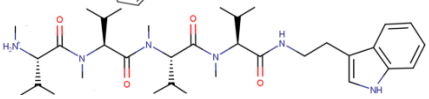

HB 378

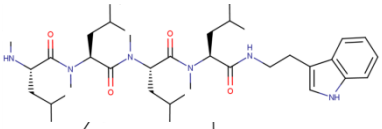

HB 528

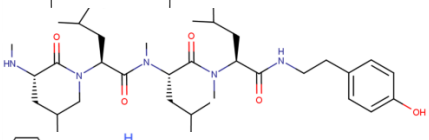

HB 531

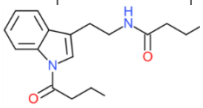

HB 602

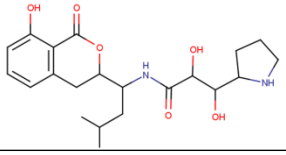

S4 Fig

PEA compound	Structure
Ph 1	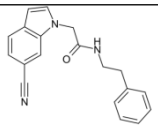
Ph 2	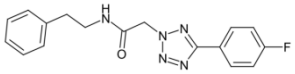
Ph 3	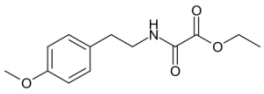
Ph 4	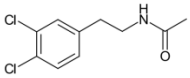
Ph 5	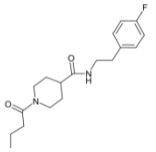
Ph 6	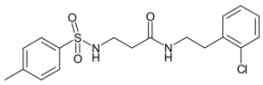
Ph 7	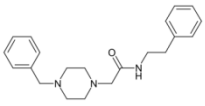
Ph 8	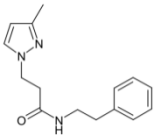
Ph 9	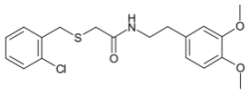
Ph 10	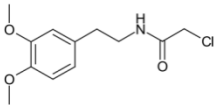
Ph 11	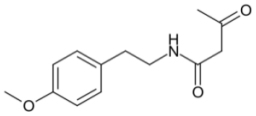
Ph 12	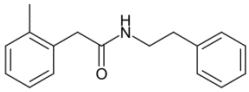

PEA compound	Structure
Ph 24	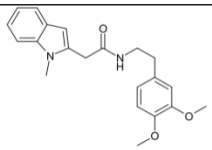
Ph 25	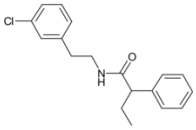
Ph 26	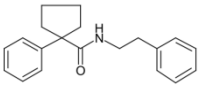
Ph 27	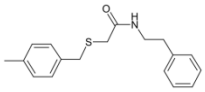
Ph 28	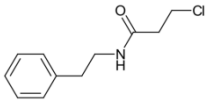
Ph 29	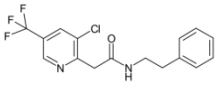
Ph 30	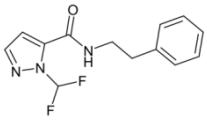
Ph 31	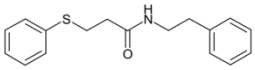
Ph 32	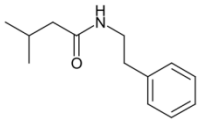
Ph 33	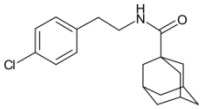
Ph 34	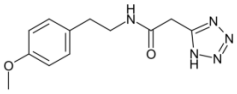
Ph 35	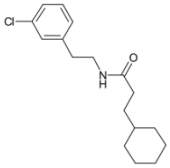

Ph 13

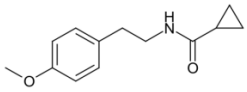

Ph 14

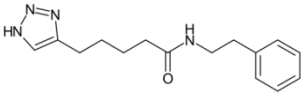

Ph 15

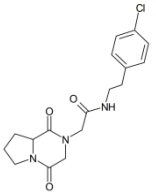

Ph 16

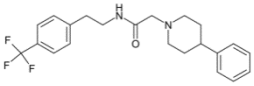

Ph 17

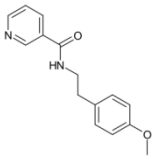

Ph 18

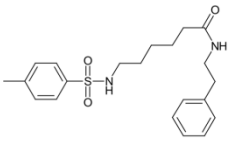

Ph 19

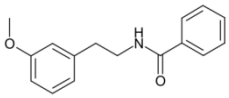

Ph 20

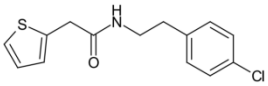

Ph 21

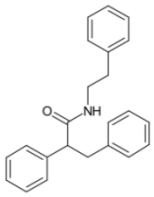

Ph 22

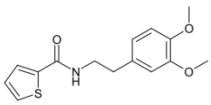

Ph 23

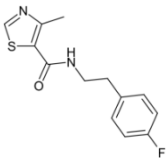

Ph 36

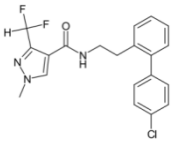

Ph 37

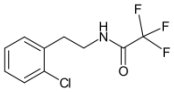

Ph 38

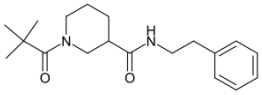

Ph 39

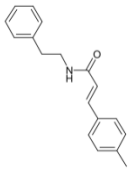

Ph 40

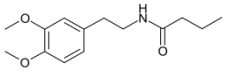

Ph 41

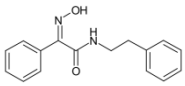

Ph 42

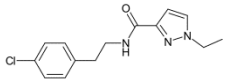

Ph 43

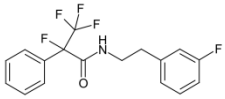

Ph 44

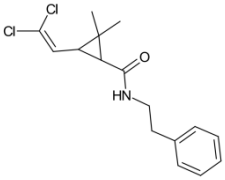

Ph 45

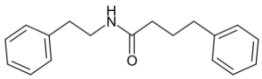

S5 Fig

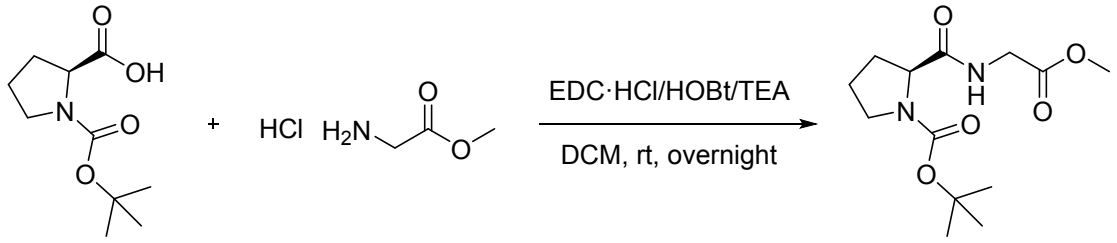

Step 1

Synthesis of (*S*)-(-)-*N*-(*t*-butoxycarbonyl)-prolylglycine methylester (**3**)

To a solution of (S)-(-)-N-(t-butoxycarbonyl)-proline **1** (5.00 g, 23.0 mmol) in CH_2Cl_2 (150 mL), amino acid methyl ester hydrochloride **2** (2.89 g, 23.0 mmol), 1-[3-(dimethylamino)propyl)]-3-ethylcarbodiimide hydrochloride (5.34 g, 28.0 mmol), and 1-hydroxybenzotriazole monohydrate (3.77 g, 28.0 mmol) triethylamine (6.50 mL, 46.6 mmol) were added and the reaction mixture was stirred for 24 h at room temperature. The solvent was removed under reduced pressure. The residue was taken up in ethyl acetate (200 mL) and washed successively with water (200 mL), 1N HCl aqueous solution (200 mL), and sat. $NaHCO_3$ aqueous solution (200 mL). The solvent was removed under reduced pressure to give (*S*)-(-)-*N*-(*t*-butoxycarbonyl)-prolylglycine methylester **3** as a white solid (4.82 g, 73%).

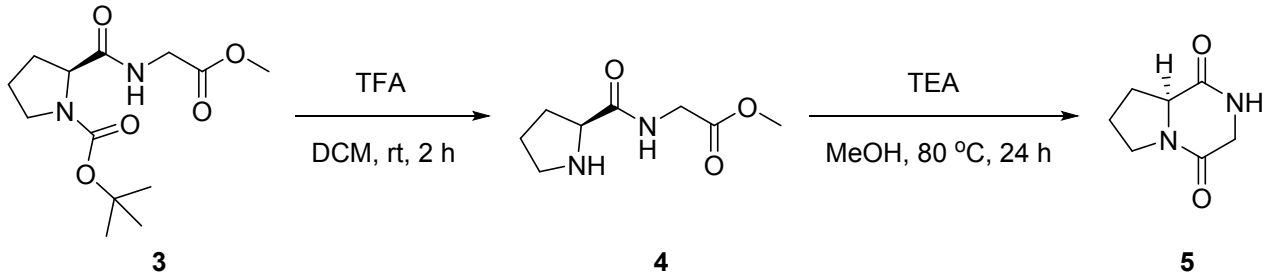

Step 2

Synthesis of (*S*)-Hexahydropyrrolo[1,2-*a*]pyrazine-1,4-dione (**5**)

To a solution of (*S*)-(-)-*N*-(*t*-Butoxycarbonyl)-prolylglycine methylester **3** (4.80 g, 16.8 mmol) in CH_2Cl_2 (84 mL), trifluoroacetic acid (18.7 mL, 252.0 mmol) was added and the solution was stirred at room temp for 2 hr. The solvent was removed under reduced pressure. The residue was dissolved in MeOH (84 mL) and treated with triethylamine (9.3 mL, 67.2 mmol). The reaction mixture was kept under reflux overnight. The solvent was removed under reduced pressure and the oily residue was redissolved in *i*-propanol to give (*S*)-hexahydropyrrolo[1,2-*a*]pyrazine-1,4-dione **5** as a white solid (2.0 g, 78%).

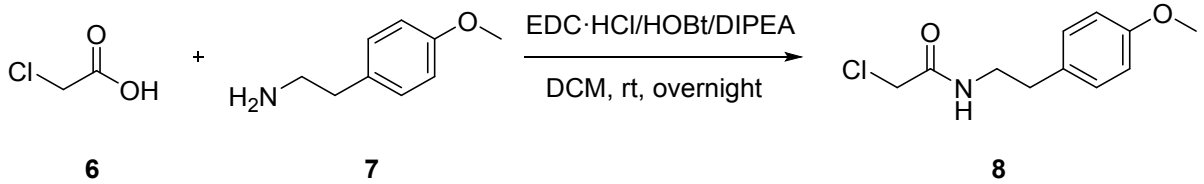

Step 3

Synthesis of 2-chloro-*N*-(4-methoxyphenethyl)acetamide (**7**)

To a solution of 2-chloroacetic acid **6** (3.00 g, 31.8 mmol) in CH_2Cl_2 (160 mL), 2-(4-methoxyphenyl)ethylamine **7** (4.6 mL, 31.8 mmol) and *N,N*-diisopropylethylamine (8.45 mL, 63.5 mmol) were added and the reaction mixture was stirred for 15 min at room temperature. After addition of 1-[3-(dimethylamino)propyl)]-3-ethylcarbodiimide hydrochloride (7.30 g, 38.1 mmol) and 1-hydroxybenzotriazole monohydrate (5.14 g, 38.1 mmol), the reaction mixture was stirred for 24 h at room temp. The reaction mixture was washed successively with 1 N HCl aqueous solution (160 mL) and sat. $NaHCO_3$ aqueous solution (160 mL). The organic layer was dried over $MgSO_4$, filtered, and concentrated. The residue was washed with diethyl ether to give 2-chloro-*N*-(4-methoxyphenethyl)acetamide **8** as a yellow solid (4.60 g, 63%).

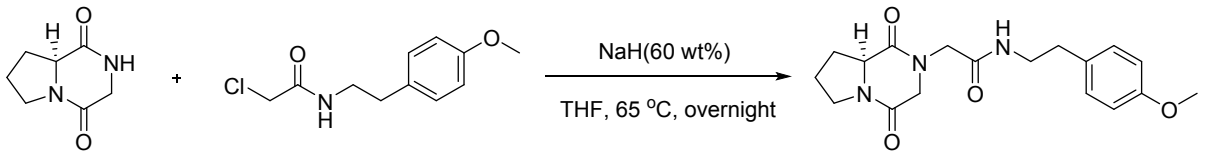

5 **8** **9**

Step 4

Synthesis of (*S*)-2-(1,4-dioxohexahydropyrrolo[1,2-*a*]pyrazin-2(*1H*)-yl)-*N*-(4-methoxyphenethyl)acetamide (**9**)

To a solution of (*S*)-hexahydropyrrolo[1,2-*a*]pyrazine-1,4-dione **5** (1.00 g, 6.40 mmol) in THF (32 mL), portionwise 60 wt% NaH (260 mg, 6.40 mmol) at 0°C was added and the reaction mixture was stirred 15 min at room temperature. 2-chloro-*N*-(4-methoxyphenethyl)acetamide **7** was added slowly to the reaction mixture then the mixture was stirred overnight at 65°C. The reaction was monitored by TLC. The reaction mixture was quenched with sat. NH_4Cl aqueous solution (100 mL) and extracted with EtOAc (2 X 100 mL). Combined organic layers were dried over MgSO4, filtered, and concentrated. The crude product was purified by silica-gel column chromatography (eluent: MeOH 10% in CH_2Cl_2) to give (*S*)-2-(1,4-dioxohexahydropyrrolo[1,2-*a*]pyrazin-2(*1H*)-yl)-*N*-(4-methoxyphenethyl)acetamide **9** as a yellow foam (1.74 g, 79%).

S6 Fig